5-2010

Study of Micro Rotary Ultrasonic Machining

Aarati Sarwade
University of Nebraska at Lincoln, sarwade.aarati@huskers.unl.edu

STUDY OF MICRO ROTARY ULTRASONIC MACHINING

by

Aarati Sarwade

A THESIS

Presented to the Faculty of

The Graduate College at the University of Nebraska

In Partial Fulfillment of Requirements

For the Degree of Master of Science

Major: Industrial and Management Systems Engineering

Under the Supervision of Professor Kamlakar P. Rajurkar

Lincoln, Nebraska

May, 2010

STUDY OF MICRO ROTARY ULTRASONIC MACHINING

Aarati Sarwade, M.S.

University of Nebraska, 2010

Adviser: Kamlakar P. Rajurkar

Product miniaturization for applications in fields such as biotechnology, medical devices, aerospace, optics and communications using a variety of materials has made the advancement of micromachining techniques essential. Machining of hard and brittle materials such as engineering ceramics, glass and silicon is a formidable task. Rotary ultrasonic machining (RUM) is one process capable of machining these materials. It is a hybrid machining process which combines the mechanism of material removal of conventional grinding and ultrasonic machining. Downscaling of RUM for micro scale machining is essential to generate miniature features or parts from hard and brittle materials.

The goal of this thesis is to conduct a feasibility study and to develop a knowledge base for micro rotary ultrasonic machining (MRUM). Positive outcome of the feasibility study led to a comprehensive investigation on the effect of process parameters on the MRUM process performance. The effect of spindle speed, grit size, vibration amplitude, tool tip geometry, static load and coolant on the material removal rate (MRR) of MRUM was studied. In general, MRR was found to increase with increase in spindle

speed, vibration amplitude and static load. The machining rate was also noted to depend upon the abrasive grit size, tool tip geometry. During the constant force mode of operation, it was difficult to maintain the force at a constant value. Therefore, a constant feedrate mode of operation was used for machining. The behavior of the cutting forces was modeled using time series analysis. It was found that the variance associated with the cutting force was least at the highest spindle speed. Capability of MRUM process for machining bone tissue was investigated. Critical issue in bone machining is the thermal damage caused to the tissue because of excessive rise in the machining temperature. Being a vibration assisted machining process, heat generation in MRUM is low and therefore it is a potential option for bone machining. Finally, to estimate the MRR a predictive model was proposed. The experimental and the theoretical results exhibited a matching trend.

ACKNOWLEDGEMENTS

I am extremely grateful to my adviser, Prof. K. P. Rajurkar, for his generous and patient support throughout the duration of my Master's study. I would like to thank him for giving me the opportunity to work at Center for Nontraditional Manufacturing Research. It was a very enriching experience both professionally and personally. His dedication to research, persistence and discipline has been a constant source of motivation.

I wish to thank Dr. M. M. Sundaram for his guidance during the progress of this thesis. His invaluable inputs, constant support and time spent are gratefully appreciated.

I thank Dr. Fred Choobineh and Dr. Jerald Varner for taking the time to be on my thesis defense committee. Their valuable comments and insights are appreciated.

I wish to thank Dr. Xingzhong Li from NCMN facility and John Bruce from Dr. Alexander's lab in Electrical Engineering department for their help with the Scanning Electron Microscope.

I thank my friends and colleagues at CNMR for making my stay in Lincoln enjoyable and a very good learning experience.

I express my gratitude towards my parents for their love and constant encouragement. They had a great influence on my academic choices and career path. Finally, I dedicate this thesis to my late grandfather who was always very encouraging and supportive of my graduate education.

TABLE OF CONTENTS

LIST OF FIGURES

LIST OF TABLES

CHAPTER 1

INTRODUCTION

1.1. Needs in Micromachining

Innovations in the fields of biomedical devices, aerospace, automobile, energy, optics, semiconductors, electronics and communications have led to miniaturization of the parts and devices. Small sized devices and their component parts are desirable to keep things compact and portable. Therefore, material and energy required for manufacturing reduces drastically. As a result the cost of production and environmental pollution is reduced. Small parts have lower inertia because of which production process needs lesser time. Consequently, the productivity increases.

Production of small parts requires different processes and systems capable of machining at micro scale [1]. To manufacture functional micro parts and devices, tighter tolerances, higher accuracy and precision, superior surface integrity, improved repeatability and reliability are desirable constantly. These capabilities are limited by the existing technology. Consequently, constant advancement of the micro machining techniques is essential for fabrication of the micro parts and devices.

Micro machining is defined as the ability to produce features with the dimensions between 1 μm to 999 μm [2] or when the volume of the material removed is at the micro level (e.g. micro grinding).

Research in micro-manufacturing focuses on developing techniques for machining materials including electrical discharge machining (EDM), electrochemical machining

(ECM), laser, ultrasonic machining. The machinability of the materials used for making the devices and parts depend on their characteristic properties. Some materials such as ceramics, titanium alloys are difficult to machine by the traditional machining techniques because of their high hardness and toughness. Nontraditional machining techniques including ultrasonic machining and rotary ultrasonic machining can be used to machine such hard and brittle materials. Some of the applications of typically used hard and brittle materials are listed in the Table 1.1.

Table 1.1. Applications of hard and brittle materials [3]

Materials	**Applications**
Glass	Micro-fluidic systems ; accelerometer ; monolithic grid structure ; lab-on-chip; micro device for blood analysis ; membrane in fuel cell
Quartz Crystal	Accelerometer; optical chopper ; pressure sensor ; acoustic wave resonator, filter, and sensor
Lead Zirconate Titanate (PZT)	Actuators and transducers ; medical imaging transducers
Silicon Carbide	High temperature pressure sensor ; vibration sensor ; micro-gas turbine engine ; micromotors operating up to 500^{o}C
Silicon Nitride	Biaxial pointing mirrors; solid immersion lens
Alumina	Micro gimbal ; bilayer lipid membranes sensor ; vacuum windows

1.2. Rotary Ultrasonic Machining

Rotary Ultrasonic Machining is a nontraditional manufacturing technique for machining hard and brittle materials such as titanium alloys [4] and ceramics [5]. These materials are hard to machine by conventional techniques such as drilling, milling,

turning and expensive to machine by other non conventional techniques such as laser and EDM. RUM offers a convenient and inexpensive way of machining these hard and brittle materials. The RUM process involves material removal by hybrid action of ultrasonic machining (USM) and conventional grinding.

The setup for RUM consists of an ultrasonic spindle kit, feeding device and a coolant system. A rotating and ultrasonically vibrating abrasive bonded tool is fed towards the workpiece. The tool removes material from the workpiece because of the ultrasonic impacts and the grinding action of the abrasives. RUM has been used to machine materials such as alumina [5, 6], beryllium oxide [7], canasite [8], composites [8, 9], ferrite [10], glass [11], polycrystalline diamond compact [12], silicon carbide [13], silicon nitride [14], zirconia [15, 16], titanium alloys [4], and stainless steel [17].

RUM was developed as an improvement over ultrasonic machining (USM). USM uses abrasive slurry (essentially a mixture of abrasive and coolant) which is fed between an ultrasonically vibrating tool and the workpiece during machining. In RUM, the loose abrasives are abandoned and are bonded to the tool itself. As a result, some of the disadvantages of the ultrasonic machining were overcome in RUM. For example, in the presence of the abrasive slurry, the escaping debris and the suspended abrasive particles tend to erode the walls of the machined hole during flushing thus making it hard to hold close tolerances. The use of diamond impregnated tool was reported to improve the hole accuracy and it was easier to drill deeper holes. It is not always desirable to expose the workpiece to the abrasive slurry; consequently, with the abandoning of the abrasive slurry, RUM could be extended to a wider range of applications. RUM was reported to be

capable of machining ten times faster than USM under similar conditions. A superior surface finish and a low tool pressure could be achieved compared to USM [18].

1.3. Micro Rotary Ultrasonic Machining

The advantage of rotary ultrasonic machining for machining hard and brittle materials is clearly evident from the discussion in the previous section. Till date RUM has been developed and well researched only at the macro level. Downscaling of RUM is essential for machining micro parts and micro features in hard and brittle materials. Hence, in the present research feasibility of MRUM has been explored. Major issues involved in the downscaling of RUM are discussed below. Two major requirements for MRUM are the micro sized abrasive bonded tool and a machining system capable of applying very small load on the micro tool with necessary feedback and control mechanisms.

1.4. Research Objectives

Rotary Ultrasonic Machining has been extensively researched at the macro level with regard to the effect of machining parameters. However, downscaling of RUM to micro level is essential to produce miniature features or parts of hard and brittle materials.

The goal of this thesis is to conduct a feasibility study and develop a knowledge base for micro rotary ultrasonic machining (MRUM). For achieving this goal the following research objectives were set.

The first objective of this thesis is to downscale rotary ultrasonic machining for micro scale machining.

The second objective is to perform parametric studies to evaluate the effect of process parameters on MRUM performance by experimentation.

The third objective is to understand the mechanism of material removal and tool wear.

The fifth objective is to develop and verify a predictive model for MRR of MRUM.

1.5. Thesis Organization

Chapter 2 presents a literature review of the rotary ultrasonic machining describing the process mechanism, equipment evolution, and previous research conducted on the parametric studies. Micro ultrasonic machining (MUSM) process, its advantages and limitations are also described. This is followed by an introduction to micro rotary ultrasonic machining (MRUM).

Chapter 3 includes the details of the in-house designed and built equipment, tooling, machining parameters selected and the experiments performed.

Chapter 4 explains the results and presents a discussion for the experiments conducted using the PCD tool and electroplated abrasive bonded tool. The effect of process parameters on the machining performance is discussed. SEM images were used to understand the material removal mechanism and tool wear.

Chapter 5 presents a literature review on the need for machining bones and investigates the possibility of using MRUM for drilling holes in a section of bone.

Chapter 6 presents the development of a predictive model for material removal rate in MRUM, followed by the verification of the model.

Chapter 7 presents the analysis of the cutting force using time series analysis in an attempt to control the process and understand the process mechanism.

Chapter 8 presents a summary of the major contributions from this study and recommendations for future research.

CHAPTER 2

LITERATURE REVIEW

2.1. Introduction

This chapter describes the rotary ultrasonic machining (RUM) process and evolution of the process in sections 2.2 and 2.3. It reports the current research on the mechanism of material removal and machining parameters in sections 2.4 and 2.5. The evolution of the machining system used for RUM is described in section 2.6. The theoretical models developed for RUM process are summarized in section 2.7. Section 2.8 elaborates on development of micro USM and discusses the challenges faced in downscaling the process. Section 2.9 discusses the MRUM process.

2.2. Rotary Ultrasonic Machining (RUM) Process

Rotary Ultrasonic Machining (RUM), by definition, is a hybrid machining process where the ultrasonic machining and conventional grinding occur simultaneously to remove material from the workpiece by micro chipping and grinding action of the abrasives. The setup for RUM consists of a rotating and ultrasonically vibrating diamond abrasive studded tool which is fed towards the workpiece such that a constant pressure or a constant feedrate is maintained during machining. A coolant injected between the tool and the workpiece through a hollow tool flushes away the debris. RUM has also been referred to as Ultrasonic Impact Drilling [19] and Ultrasonic Vibration Assisted Grinding [20].

A workpiece for RUM is usually characterized by properties of high hardness and brittleness. Thus, machinability of a material is independent of its other material properties such as electrical conductivity and chemical reactivity. RUM is a non-thermal, non-chemical and non-electrical process. As a result the metallurgical, chemical or physical properties of the workpiece do not change post machining [21]. Virtually a stress free surface is generated after machining, thus, the fatigue strength of the machined material does not deteriorate. RUM has been used for drilling and coring [22]. It has also been extended to milling [14, 23], disk grinding [24] and contour machining [25].

2.3. Evolution of RUM

Literature reports that RUM was developed as an improvement over ultrasonic machining (USM) [18]. Unlike USM, instead of using the loose abrasive slurry, the diamond abrasives were impregnated into the rotating tool. Typically RUM was used for drilling holes through hard and brittle materials. The development of RUM as a successor of ultrasonic machining (USM) is discussed in this section. USM was patented in 1927 and has been used in the industry since 1940 for machining materials with high hardness and brittleness. This process uses abrasive slurry (essentially a mixture of diamond abrasives and a cooling fluid) which is fed between an ultrasonically vibrating tool and the workpiece during machining. P. Legge developed RUM for the first time in 1964. The schematic diagram in Figure 2.1 illustrates the principle of ultrasonic machining as the abrasive slurry is injected in between the tool and the workpiece. Figure 2.2 illustrates the schematic diagram of RUM.

Advantages of RUM over USM: Some of the disadvantages of the ultrasonic machining were overcome in RUM. In the presence of the abrasive slurry, the escaping debris and the suspended abrasive particles tend to erode the walls of the machined hole during flushing thus making it hard to hold close tolerances. The use of diamond impregnated tool was reported to improve the hole accuracy and it was easier to drill deeper holes. It is not always desirable to expose the workpiece to the abrasive slurry. Consequently, on abandoning of the abrasive slurry, RUM could be extended to a wider range of applications. RUM was reported to be capable of machining ten times faster than USM under similar conditions. A superior surface finish and a low tool pressure could be achieved compared to USM [18].

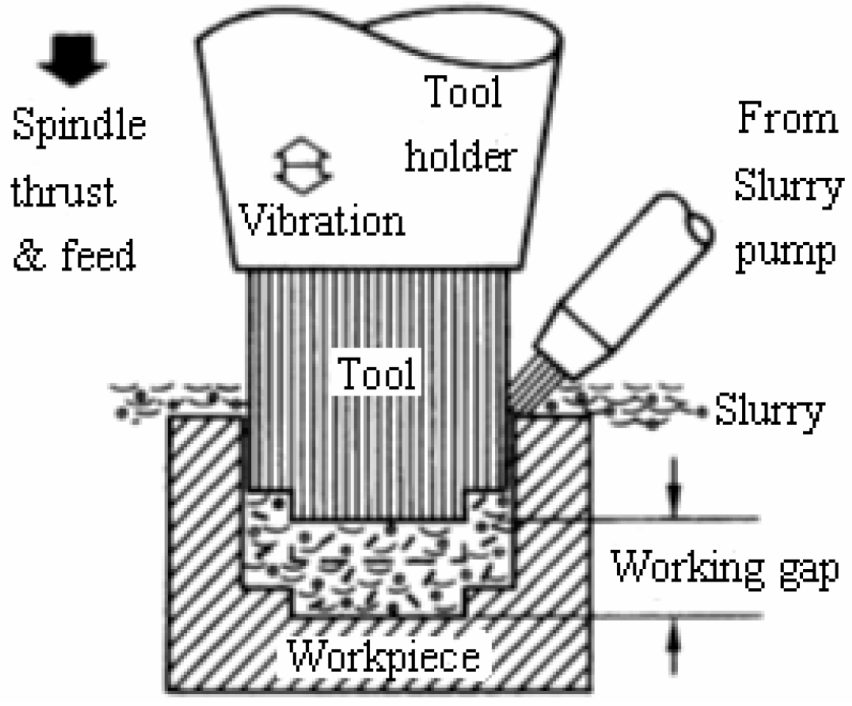

Figure 2.1. Illustration of ultrasonic machining [26]

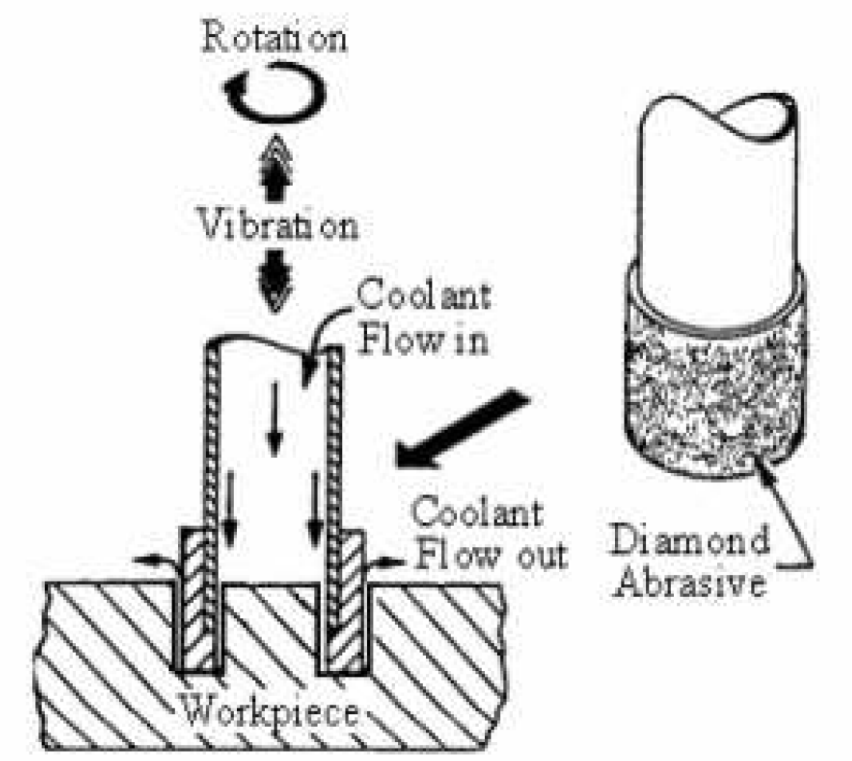

Figure 2.2. Illustration of rotary ultrasonic machining [26]

2.4. Mechanisms of Material Removal

The mechanism of material removal has been investigated by studying the surface topography of the machined surface and mechanisms involved in the single grit scratching experiments [27, 28]. Dominant mode of material removal was due to brittle fracture. The impact, grinding and erosion generated by tool rotation and vibration were responsible for the brittle fracture [28, 11]. The impact was found to be a major factor for material removal towards the tool tip, while grinding was dominant near the walls of the hole. The debris produced due to impact and grinding mixed with the pressurized coolant were responsible for erosion at the hole walls during machining. Ductile mode of material removal also contributed towards machining [16].

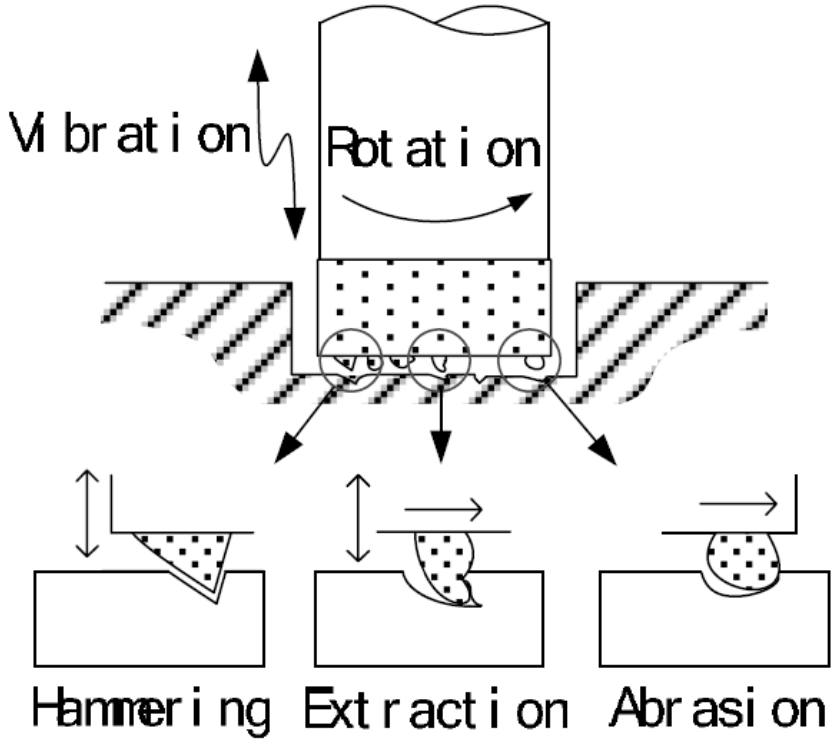

Figure 2.3. Material removal modes in RUM [29]

In recent studies, the advantages of ductile regime machining of brittle materials were emphasized [30]. Minimal subsurface damage and better surface finish are the results of ductile regime machining. Ductile machining is based on the fact that all materials deform plastically if the degree of deformation is small enough. There exists a critical depth of indentation for the abrasive grits involved. If the applied force on the abrasive grain exceeds this critical value, cracks are developed in the workpiece. However, if this depth of indentation is below the critical depth, material is removed by plastic flow [30]. During ultraprecision diamond turning, as the tool traversed across the workpiece, zones of machining were formed as the tool traverses across the workpiece:

(i) a ductile zone where continuous chips are formed and the surface defects such as micro-cracks and craters are absent (ii) a ductile-brittle-transition zone where the surface is semi-brittle fractured and (iii) a brittle fractured surface where holes, cracks and severe surface damage can be observed [31]. Figure 2.4 illustrates the three zones of machining.

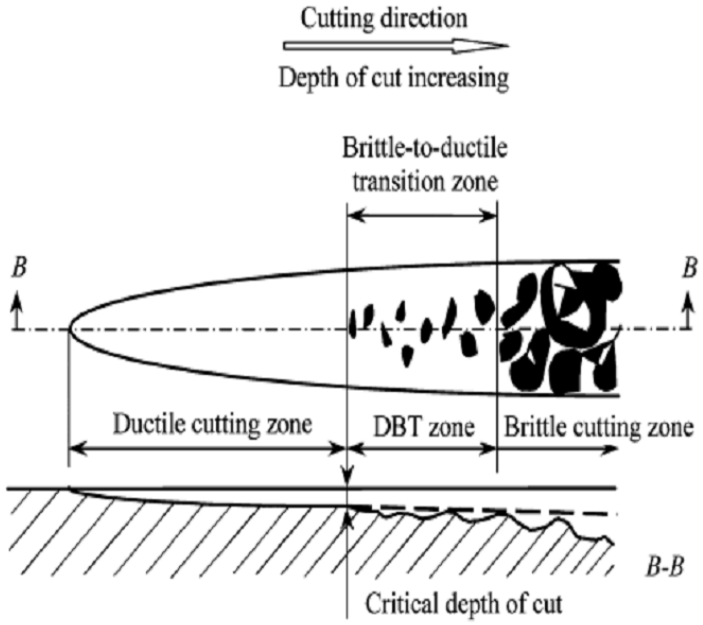

Figure 2.4 Schematic diagram of ductile-regime machining [31]

Experiments with single point diamond tool reveal that the use of ultrasonic vibrations increased the critical depth of cut to a higher value allowing ductile (plastic flow) machining to occur up to a higher value. The reduction in the cutting forces and frictional forces as a result of using the ultrasonic vibrations was proposed to be a reason for this increased value of the critical depth of indentation [32]. This phenomenon has also been observed for ultrasonic assisted grinding of nano ZrO_2 ceramics [33]. The

critical chip thickness has been defined as a function of material properties. The process parameters and tool geometry are also important factors in ductile-regime machining [31].

2.5. Machining Parameters

The machinability of materials such as titanium alloy [4, 34], advanced ceramics [5, 18, 26], ceramic matrix composites [9], silicon carbide [13], stainless steel [17], dental ceramics [35], potassium dihydrogen phosphate [36], glass [11] is investigated under different machining conditions in the recent years.

A summary of literature regarding the effect of different machining parameters on material removal rate (MRR), average surface roughness, tool wear and edge chipping is presented in the following sections.

2.5.1. Material removal rate

MRR was found to increase with an increase in the machining pressure [18], increase in the feedrate, at a higher spindle speed [18, 4] and with increase in ultrasonic frequency [19]. Vibration amplitude was found to have a significant effect on the MRR [18]. With increase in abrasive grit size and abrasive concentration, MRR was found to increase upto a certain optimal value and then a decreasing trend was observed [18, 37]. During RUM of ceramics, MRR reduced as the strength of the bond increased [18]. The type of coolant (oil or water) did not affect the MRR [38].

2.5.2. Cutting force

The cutting force was observed to reduce as the spindle speed was increased [4, 5, 13, 17, 18] and feedrate was decreased [5, 9, 13, 18] during RUM of different materials. Ultrasonic vibration power had significant effect on the cutting force [4, 17]. Lower cutting forces were produced when a larger abrasive grit size, a higher abrasive concentration [34] and water-based coolants were used compared with synthetic coolants or tap water. [39].

2.5.3. Surface roughness

Surface roughness was found to reduce with decrease in machining pressure, decrease in feedrate [18], decrease in ultrasonic vibration frequency [19] and at a higher spindle speed [4, 9]. A nonlinear dependence of ultrasonic power on the surface roughness was observed while machining ceramics. A reduction in average surface roughness was found with increase in ultrasonic power while machining two metals including stainless steel and titanium alloy [4, 13]. With increase in abrasive grit size the surface roughness increases upto a certain value and then decreases [18, 34]. Natural diamond was observed to reduce the surface roughness compared to the synthetic diamond abrasive [18]. A high abrasive density led to a decreased surface roughness. However, if the abrasive density is very high, the strength of the abrasive layer is reduced, leading to an increased tool wear and thus higher surface roughness [37]. Coolant pressure affected the surface roughness significantly [39].

2.5.4. Tool wear

Accuracy and surface finish of the machined feature are affected as the tool wears out. It is therefore important to understand the mechanism and the influence of machining

parameters on tool wear. In RUM, the wear of tool was calculated as specific tool wear which was defined as the ratio of the volume of the material removed to the volume of the tool wear. Specific tool wear provides no information on the mechanism of tool wear [19]. In an investigation of the tool wear mechanism in silicon carbide, attritious tool wear and bond failure, similar to those in grinding, were observed. Tool wear at the end face was more severe than the tool wear at the lateral face. Correlation of the tool wear with cutting forces was proposed to be used for online monitoring of the tool wear [40]. In another study, acoustic emission signals were used to assess the wearing patterns of the tool for monitoring purposes [41]. The influence of different tool variables including grit size, metal bond type, and diamond concentration on the tool wear during machining of titanium alloy were studied [34].

2.5.5. Edge chipping

Finite element models were developed to study the edge chipping and cutting forces during machining of ceramics. The results were compared with the experimental data. A higher spindle speed and lower feedrate resulted in a lower chipping thickness because of the reduced cutting forces [42]. Efforts were made to reduce the edge chipping in a further study [43]. It was found that on increasing the support length (the radial length of contact area between workpiece and the fixture) and decreasing the cutting force the edge chipping thickness decreased [44].

2.5.6. Machining temperature

The grinding temperatures were found to reduce significantly when grinding with the aid of ultrasonic vibrations. In a study of tool wear, it was found that the surface color of the diamond grains changed after machining. This implied that the surface temperature

of the diamond grains was high [40]. However, study focusing on the temperature changes during machining has not been conducted yet.

2.6. System Evolution

A typical RUM setup consists of a machine and a tool. The main components of a RUM machine are a feeding device, ultrasonic spindle kit, and a coolant system. Studies discussing variations/ developments of these components are summarized.

2.6.1. Tools

Most of the studies make use of a cylindrical tool with a through hole in its centre for supplying the coolant to the working gap. A slotted diamond tool was used in one of the studies. Surface roughness improved compared to conventional RUM with cylindrical tool. No significant difference in cutting force was observed [45]. Electroplated tools and diamond impregnated tools have been used for RUM, however, electroplated tools wore out faster even if material removed by them is at a greater rate [37, 44].

2.6.2. Feed mechanism

Two types of feed mechanisms, either a tool-down feeding or workpiece-up feeding have been used [44, 45]. Either constant feedrate or constant force/pressure control are usually employed for controlling the feed mechanism in the process. A step-back feed mechanism, involving forward-stepping the tool followed by a small back-stepping helped in efficient debris removal [46].

2.6.3. Ultrasonic vibrations

A method was developed for designing a horn for transmission of ultrasonic vibrations using the finite element method [47]. The ultrasonic vibrations are applied

along the axis of the tool and perpendicular to the plane of the tool rotation so that the abrasive grains bonded to the tool impact the workpiece. The ultrasonic vibrations can be applied either to the tool or the workpiece. While drilling using a diamond impregnated tool, ultrasonic vibrations were applied to the tool and low-frequency vibrations were applied to the workpiece. When vibrations were applied to both, the tool and the workpiece, the cylindricity error and edge chipping were reduced [48].

In another experimental study, a recently developed very high frequency ultrasonic transducer (400 kHz) was used for micro ultrasonic grinding. The spindle rotating the tool was vibrated at the ultrasonic frequency during boring of glass, ferrite and alumina. This transducer provided longitudinal, torsional, and complex (longitudinal and torsional) modes of vibration. Use of complex modes of vibration (longitudinal and torsional) resulted in the best performance due to reduced chipping and stabilized grinding force. The amplitude of vibration was kept constant by a feedback control mechanism so that the depth of cut was maintained constant at a submicron level [46].

2.6.4. Coolant system

In an innovative coolant system developed, the effect of coolant flow (continuous or intermittent) was investigated. The intermittent flow removed the debris efficiently resulting in a better performance [49].

2.7. Theoretical Work

Theoretical models were developed for predicting MRR in RUM based on brittle fracture [6, 50, 51] and ductile flow [16]. A physics based model was developed for predicting the cutting force while machining at a constant feedrate [20].

2.8. Micro Ultrasonic Machining (MUSM)

Ultrasonic machining (USM), the precursor of Rotary Ultrasonic Machining, was scaled down from macro level to micro level in mid 1990's. Figure 2.5 illustrates the principle of USM.

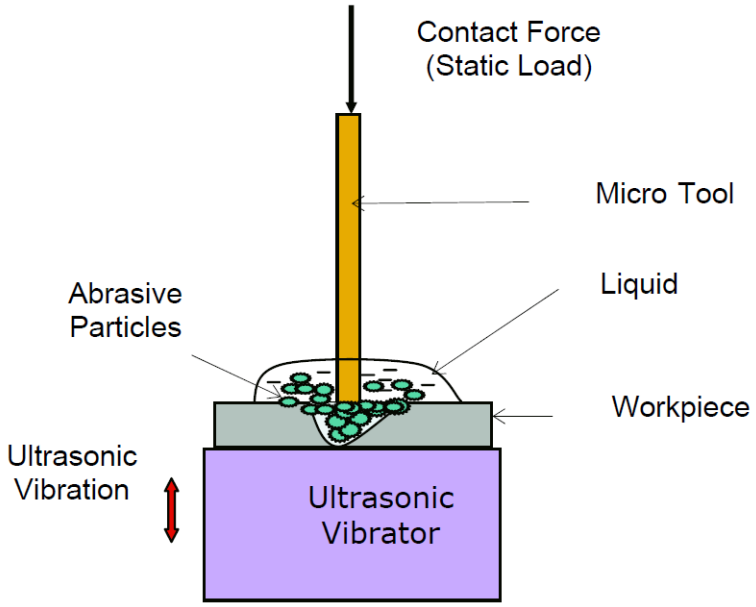

Figure 2.5. Principle of micro USM based on "vibration of workpiece" (Type-I) [41]

Since then a lot of research has been done with regard to parametric studies. It is shown to be capable of machining intriguing micro features on materials such as glass, quartz, diamond, ceramics, and semi-conducting materials [52]. There are two modes of operation of MUSM Type 1 and Type 2. Examples of features machined by the two modes are illustrated in Figure 2.6. Figure 2.6 (a) illustrates complex micro feature machined in a silicon wafer. This feature was created by using CAD/CAM method and the motion of the micro tool was controlled along the three axes to follow a designed tool path. Complex shaped features can be machined by Type 1 MUSM. Figure 2.6 (b)

illustrates micro feature machined by die sinking MUSM. In die sinking micro USM, the mirror image of the micro features desired to be machined are fabricated at the tool bottom. The tool approaches the workpiece as a die and imprints the micro feature on the workpiece. Fabrication of complex features on the micro tool face is difficult and cumbersome. However, batch production of simple features with low aspect ratio is possible with die sinking micro USM.

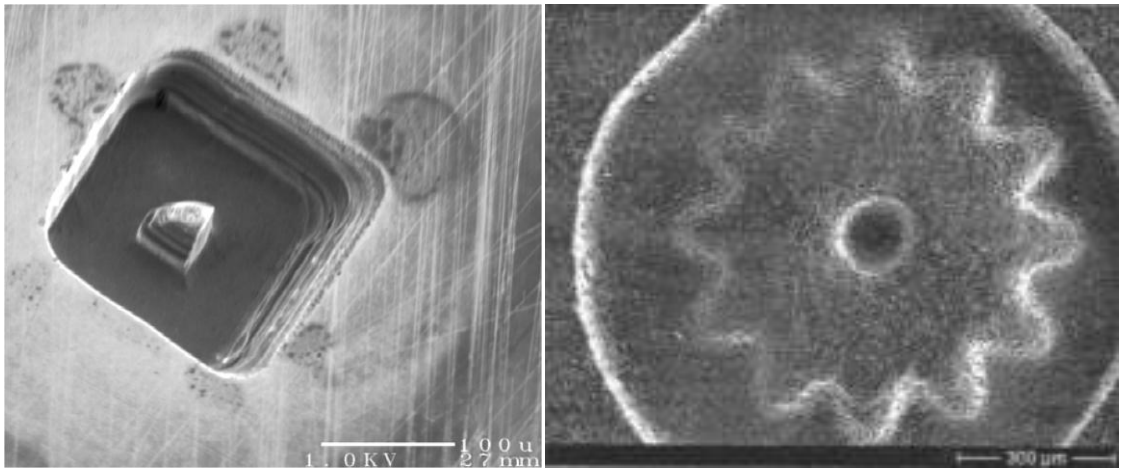

Figure 2.6. Features machined using micro ultrasonic machining: 3-D cavity [52] (a), die-sinking micro USMed feature in alumina [53] (b)

For evaluating the process performance under different machining conditions extensive parametric studies were conducted [52]. Effect of parameters such as static load, vibration amplitude, and slurry concentration were conducted [52, 54]. Theoretical models are also developed for predicting the material removal in micro USM [52, 54].

Micro Ultrasonic Machining has numerous advantages for machining hard and brittle materials. It is capable of die-sinking and contouring to fabricate complex 3D features, low cost, simple machine structure, no significant change of physical and chemical properties such as heat-affected zone (thermal damage).

However, it has some limitations which include the following

- relative low machining speed compared to the cutting processes,
- machining gap impairs dimensional accuracy,
- slurry has to be fed to and removed from the gap between the tool and the workpiece. As a result, the rate of material removal reduces and even stops as the feedrate increases,
- considerable tool wear occurs in machining and difficult tool wear compensation [52].

As reported in section 2.2 some of these limitations were also prevalent in USM at macro level. The limitations such as feeding abrasive slurry and low machining speed were overcome when an abrasive bonded tool was used in RUM. Similarly, it is hypothesized that MRUM might overcome the limitations of micro USM. Thus, to satisfy the need for an efficient low cost method for machining hard and brittle materials, the industrial need of higher precision, tighter tolerances and superior surface finish has lead to the feasibility study of MRUM.

2.9. Micro RUM

Attempts have been made to scale down RUM to a micro level. A micro USM setup was employed for machining. In the experimental study conducted, MRR was found to increase with an increase in the static load and spindle speed like macro RUM. An increase in MRR was observed with a decrease in the abrasive grit size. At larger amplitude the MRR was almost the same for all grit sizes. Chipping at the hole edges was greater when a bigger abrasive size was used. Although silicon workpiece was used

which is brittle, there was evidence of ductile machining in the form of circular concentric grooves on the drilled surface in all the experiments. The number of these grooves was different for different experimental conditions, indicating the dependence of material removal by plastic flow on machining parameters. Stick-slip marks were observed on walls and the bottom of the machined holes and on the binding metal on the tool. Tool wear was observed in the form of grain pull-out and grain fracture. Figure 2.7 shows the cause – and - effects diagram for the MRUM process. The process parameters which affect the quality of machining and tool wear are illustrated.

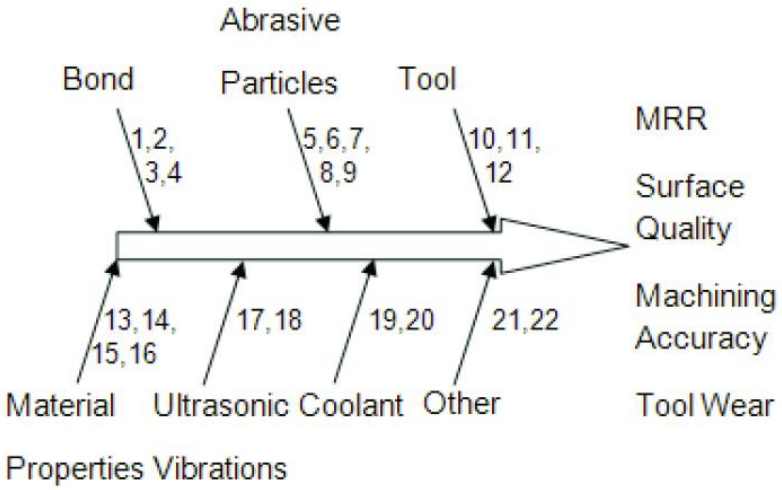

1	Bond type	12	Tool rotation speed
2	Strength of binder	13	Young's modulus
3	Porosity	14	Hardness
4	Abrasive concentration	15	Fracture strength
5	Size of abrasives	16	Toughness
6	Type of abrasives	17	Amplitude
7	Slurry concentration	18	Frequency
8	Size distribution	19	Specific heat
9	Shape	20	Viscosity
10	Tool shape	21	Static load
11	Tool size	22	Temperature

Figure 2.7. Ishikawa cause-and-effects diagram for MRUM

CHAPTER 3

EXPERIMENTS

3.1. Introduction

In this chapter the in-house designed and built experimental setup is explained in section 3.2.1. The different types of tools used are explained in section 3.2.2. Section 3.3.1 describes the experimental conditions and the experiments conducted using the polycrystalline diamond (PCD) tool. Sections 3.3.2 describes the experiments conducted using the electroplated abrasive diamond tools.

3.2. Experimental Setup

3.2.1. Micro ultrasonic machine description

An in-house designed and built micro USM machine was used for performing experiments for MRUM. The system is an assembly of a piezoelectric ultrasonic transducer, a spindle for rotating the tool (Cannon LN 22, 5W, coreless DC motor) and the position of the tool was controlled in the X, Y and Z axes by a precision motion controller (Newport PM500C) with a 25 nm resolution. The workpiece was vibrated ultrasonically by mounting it on the free end of the transducer. A double sided duct tape was used to fix the workpiece on the transducer. The coolant was injected between the tool and the workpiece. To control or monitor the forces developed during machining an electronic balance was used. The response from the balance was given as a feedback to the motion controller through a RS-232 interface to control the position of the tool on the workpiece. Figure 3.1 illustrates the schematic diagram of the system. Figure 3.2 explains

the principle of operation of MRUM. Figure 3.3 shows an image of the experimental system used.

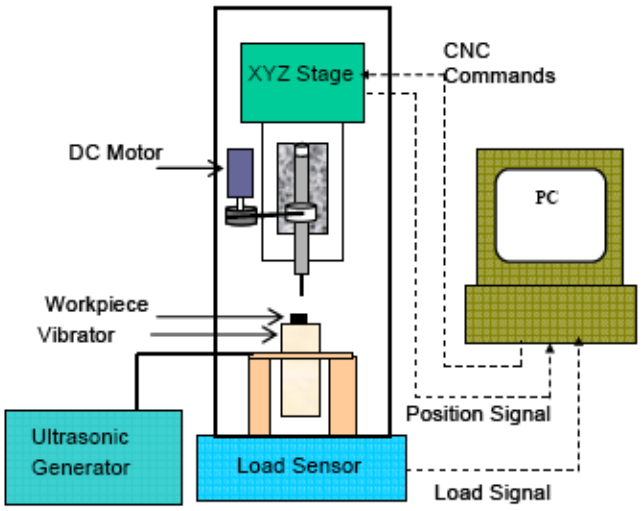

Figure 3.1. Schematic diagram of the experimental setup [52]

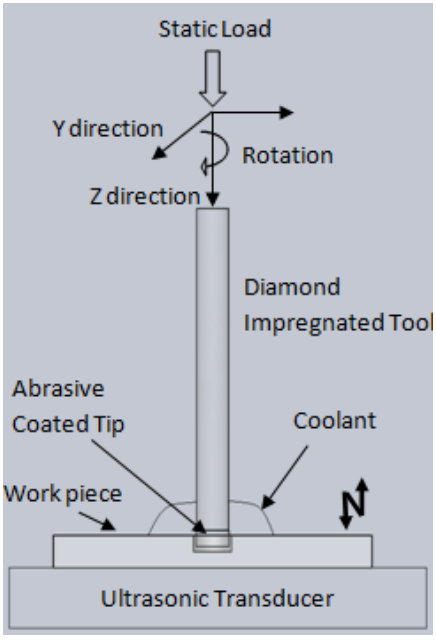

Figure 3.2. Micro rotary ultrasonic machining principle

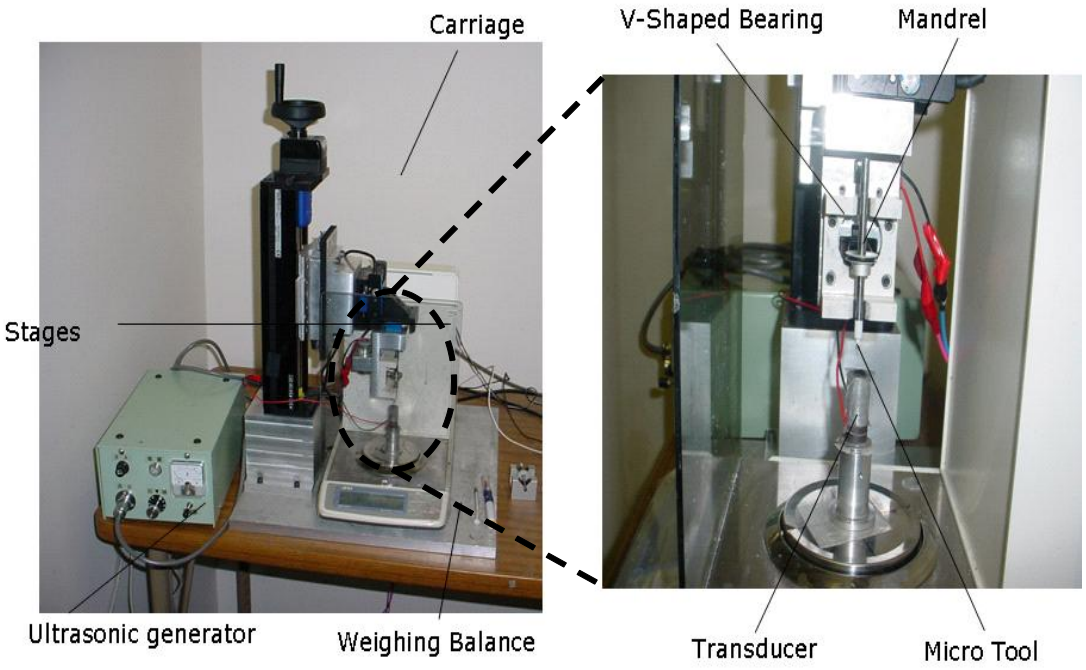

Figure 3.3. Experimental setup [52]

3.2.2. Tooling

The micro ultrasonic machining (MUSM) setup was modified to conduct the experiments. To change the MUSM setup to perform as MRUM, abrasive bonded diamond tools were used.

Initial attempts were made to fabricate the abrasive bonded tool in-house. Abrasive particles were bonded to a cylindrical micro tool with quick fix rubber adhesive. The abrasive bonded tool was dried overnight before performing the experiments. When this tool was used for machining, only few scratch marks were observed on the work surface. Figure 3.4 illustrates the images of the tool before and after machining. From the image it can be seen that the abrasive coated layer was also not perfectly cylindrical. Moreover, the abrasive coating wore off with the coolant oil. Therefore, this method of

fabricating the tool was not successful. A stronger and adherent bonding material would be able to hold the abrasive grains more effectively. Sintering or electroplating abrasives on the tool were thought to be better techniques.

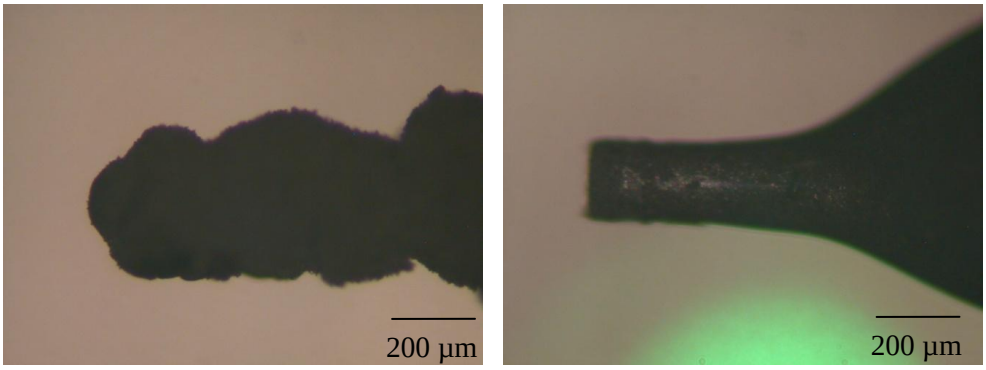

(a) **(b)**

Figure 3.4. Images of in-house made abrasive bonded tools before (a) and after machining (b)

Secondly, a PCD tool (manufactured by Sumitomo Electric) was used as the tool for MRUM. Initial attempt of machining using the PCD tool (2 mm diameter) without the abrasive slurry was unsuccessful. Machining was possible when a very high static load of the order of 80-100 g was applied on the same tool along with the usage of abrasive slurry. However, extensive heat was generated and the machining was unstable under such high static loads. Hence, for the stable machining, it was necessary to decrease the overall static load, but provide sufficient contact pressure on individual abrasive grains. Reducing the tool diameter was the best option to achieve this goal. Machining of PCD tool by conventional methods is tedious if not impossible. Wire electro discharge grinding (WEDG) from Panasonic micro EDM (MG-ED72W) was used to reduce the diameter of the PCD tool. The micro tool machined by WEDG is shown in Figure 3.5

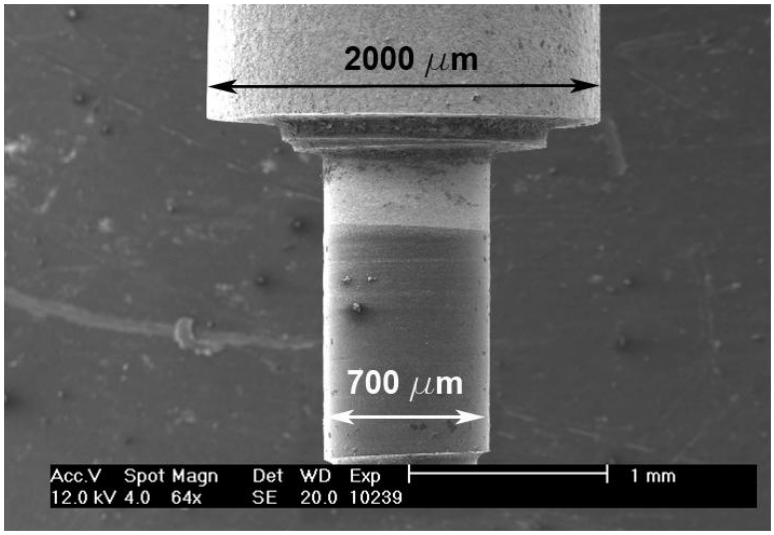

Figure 3.5. PCD micro tool made by WEDG (manufactured by Sumitomo Electric)

Thirdly, abrasive bonded tools were used for MRUM. Electroplated diamond tools (manufactured by Strauss Diamond) with different grit sizes (30~120 μm) and tool tip shapes (cylindrical and conical) were used for machining. The diamonds are plated on the tool using the HBN plating such that both the matrix and the grit are equally distributed on the tool [55]. An illustration of the tool tips with different grit sizes of 30 μm = Superfine (SF), 50 μm = Fine (F) and 107~120 μm = Medium (M) is given in Figure 3.6. The diameter of the holder available for the tool was much larger than the shaft diameter of the tool. Thus, tool after fixing directly into the holder was almost always eccentric because four screws were used to fix the tool. To ensure that the tool was centered and clamped properly into the holder, a sleeve was used. The tool was press fit into the sleeve. This assembly was inserted into the holder and the four screws were merely used to hold the tool in the appropriate position.

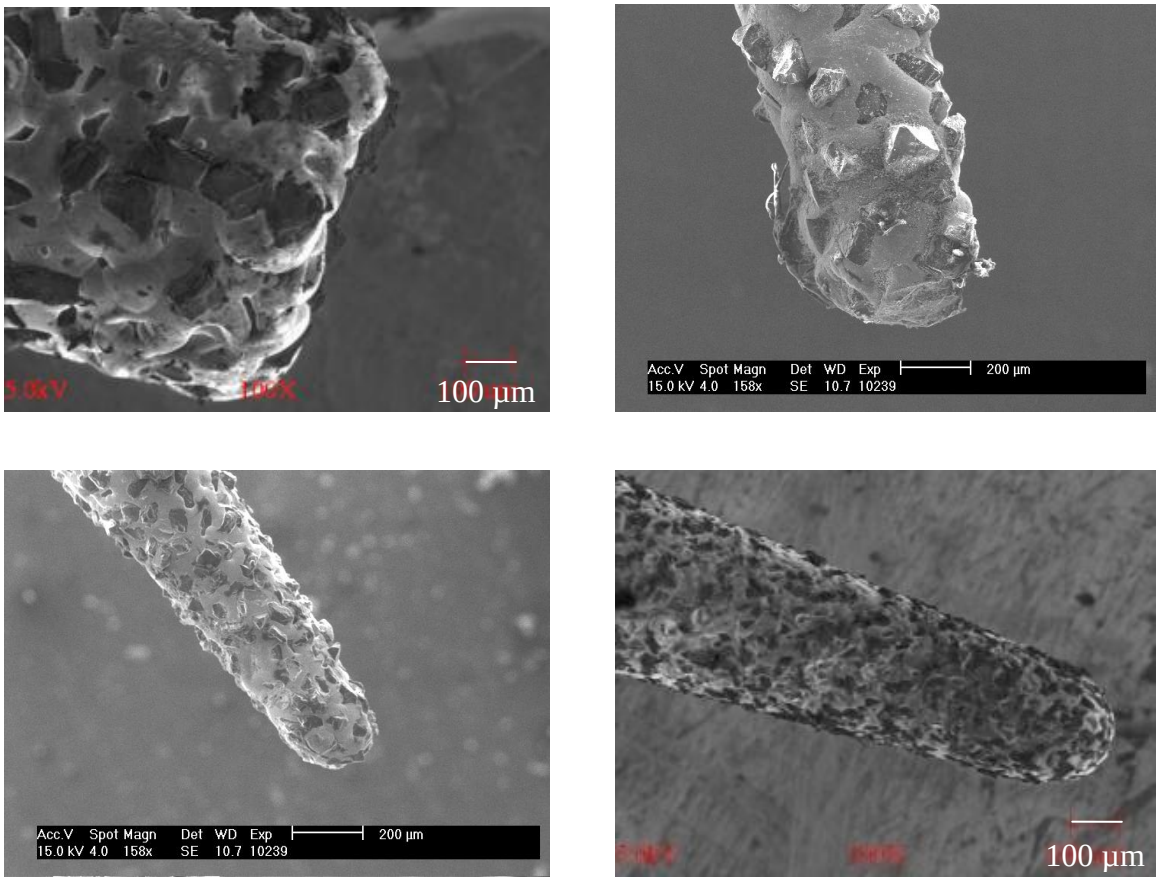

Figure 3.6. SEM images of the cylindrical tool (a) and cone shaped tools with medium (b), fine (c) and superfine grits (d) (manufactured by Strauss Diamond)

Single crystal silicon <111> wafer pieces, each weighing 0.1 g and 1 mm thick, were used as workpieces for experiments.

3.3. Plan of Experiments

The experiments conducted using the PCD tool and the electroplated abrasive tools are described in detail in this section.

3.3.1. Experiments using the PCD tool

Experiments were conducted using the PCD tool under the experimental conditions presented in Table 3.1. The experiments were conducted to investigate the preliminary effect of tool diameter, abrasive size, spindle speed and static load on MRR.

Table 3.1. Experimental conditions for MRUM using PCD tool

Tool Material	Sintered PCD
Tool Diameter	2000, 700, 500 (µm)
Work Material	Silicon wafer <1 1 1>
Abrasive Material	PCD
Abrasive Size	1-3, 3-5 (µm)
Slurry Medium	Water
Tool Rotational Speed	1000, 3000 (RPM)
Vibration Frequency	39.5 (kHz)
Vibration Amplitude	1 (µm)
Static Load	5,10,15,20 (g)

3.3.2. Experiments using the electroplated abrasive tools

3.3.2.1. Preliminary experiments

Table 3.2. Test cases

Factors	**Conditions**
Ultrasonic vibrations	on / off
Tool rotation	on / off
Dry or wet	water present or dry

To understand the individual effect of ultrasonic vibrations, tool rotation and coolant on the material removal rate, experiments were conducted in the presence and absence of each of those factors (as mentioned in Table 3.2), while the other factors were maintained at the normal machining conditions (as mentioned in Table 3.3). The results obtained for each were plotted in Figures 3.7 and 3.8.

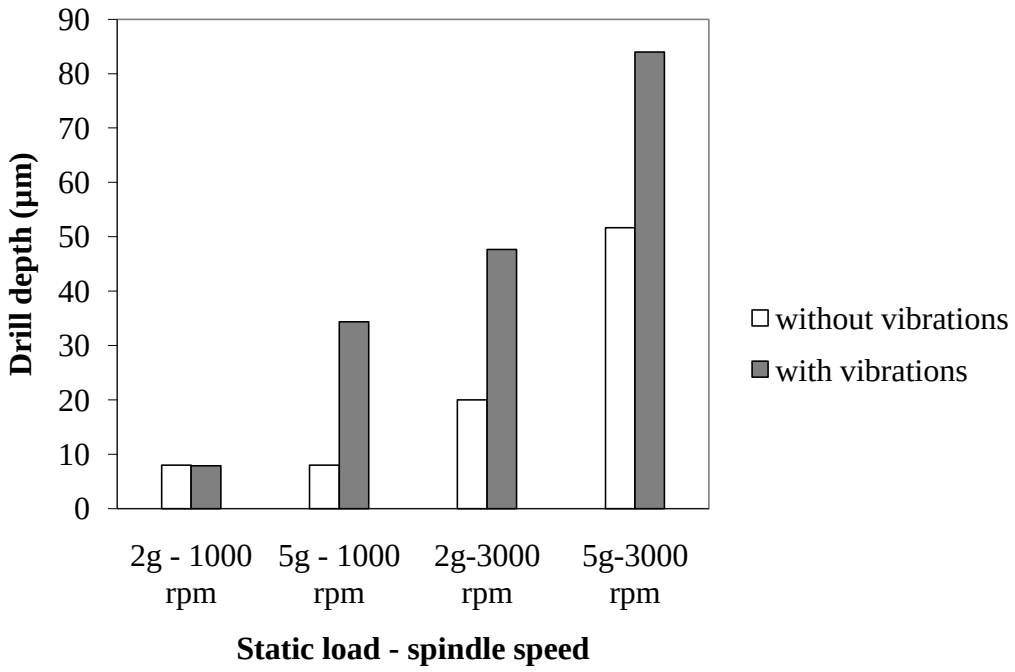

Figure 3.7. Effect of presence and absence of ultrasonic vibrations on MRR *(A = 1 µm, C = oil, G = M, t = 200 seconds)*

Ultrasonic vibrations were found to increase the drilled depth (essentially MRR) under different machining conditions as illustrated in Figure 3.7. This observation is consistent with that observed for other vibration assisted machining techniques such as vibration assisted grinding [56]. The vibrations provide an intermittent contact between the tool and the workpiece. This enables better flushing of the debris from the machining gap.

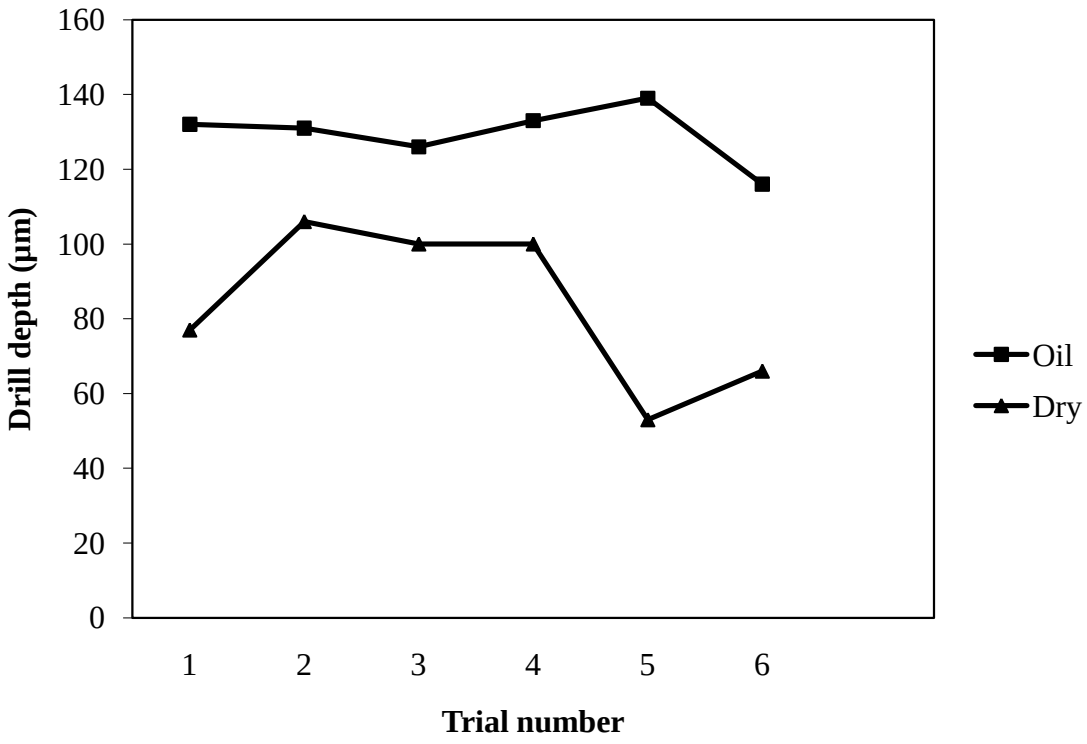

Figure 3.8. Effect of presence and absence of coolant on drill depth during machining *(A = 1 µm, G = SF, S = 3000 RPM, t = 200 seconds)*

The drilled depth was found to increase with the use of a coolant as shown in Figure 3.8. The experiments were repeated six times using one single tool under the same conditions in the presence and absence of oil. Because of the tool wear, the number of trials was limited to six. The depth of the hole achieved was same for all the trials in the presence of oil. In contrast, during dry machining, the drilled depth varied under the same machining conditions. Therefore, the process had a higher drilling speed and better repeatability of the machining rate in the presence of a coolant.

Presence of a coolant helped in removing the machined debris efficiently, even if no flushing system was used. Presence of ultrasonic vibrations aided the debris removal

from the machining gap. This provided ultrasonic cleaning as the workpiece vibrates ultrasonically. In case of dry machining the debris was removed, though not as efficiently, only because of the centrifugal force of the rotating tool and the intermittent non-contact time provided because of the ultrasonic vibrations.

The effect of the use of tool rotation in MRUM was also investigated. No machining occurred when the tool was not rotating. The presence of each of the three above mentioned factors contribute towards improving the material removal process. Therefore, all the experiments for this study were conducted in the presence of ultrasonic vibrations, coolant and tool rotation.

Table 3.3 lists all the possible parameters which were changed and the possible levels chosen during machining. Different combinations of these parameters were chosen as different sets and the experiments were conducted using the specified parameters as described below.

From the literature review, vibration amplitude, spindle speed, grit size were identified as the main parameters for study. The effect of other parameters such as coolant and static load is not known for MRUM. For MUSM static load and type of coolant used were found to have an effect on the machining process [52, 57]. To identify a suitable operating value of these parameters, experiments were conducted which are described below.

Table 3.3. Experimental conditions for MRUM using electroplated abrasive tools

Parameters	**Levels**
Abrasive Grit Size (G)	30, 50, 107~120 (μm)
Ultrasonic Vibration Amplitude (A)	1, 2.5, 4 (μm)
Spindle Speed (S)	0, 500, 1000, 3000, 5000 (RPM)
Static Load (SL)	5, 8 (g)
Coolant (C)	oil, water
Tool Tip Shape	conical (SF, F, M), cylindrical (M)
Tool Feed Mode	feedrate controlled mode, force controlled mode
Machining Time (t)	200, 400 (seconds)

The experiments were performed with cylindrical tools (diameter 800 μm, grit size M). Two different levels of static load (5 and 8 g), spindle speed (1000 and 3000 RPM) and coolant (water and oil) were chosen. Silicon wafer pieces were used as workpieces, each weighing 0.1 g and 1 mm thick, in the experiments conducted. Each experiment was conducted twice and average value of the MRR obtained was recorded. The radial dimension of the machined hole was measured from the SEM images. Hole enlargement (radius of the tool was subtracted from the radius of the machined hole) was recorded.

MRR by cylindrical and conical tool tip shapes experiments were done under the same machining conditions, with tools having the same grit size. Each experiment was conducted three times and the average value was recorded.

All the previous experiments were done using a constant force mode of operation. Prior research done on macro level RUM is mainly using the constant feedrate mode [4,

5]. To understand the trend in the machining forces developed during MRUM, the machine was operated in the feedrate controlled mode. The tool was fed towards the workpiece at a constant feedrate value. Experiments were performed at four different values of feedrates (0.04, 0.08, 0.13, 0.5 μm/s) and three values of spindle speeds (500, 3000, 5000 RPM) and the average force was recorded during machining for each experiment. Each experiment was repeated thrice and the average value of the forces thus obtained was recorded.

3.3.2.2. Main experiments

From the results and observations of the test cases and preliminary experiments, the values of the machining parameters and tool feed mode for the main experiments were selected.

The main experiments were focused on understanding the influence of grit size, tool rotation and vibration amplitude on MRR. Cone shaped tools were used for these experiments. The machine was operated in the constant force mode. The static load was kept fixed at 5 g. Five levels of spindle speeds (0, 500, 1000, 3000, 5000 RPM), three levels of abrasive grit sizes (SF, F, M) and vibration amplitudes (1, 2.5, 4 μm) were used for conducting the experiments. The effect on the MRR was measured and recorded. Material removal rate for the conical tool was calculated by assuming the tip to be made up of a hemispherical end fixed over a truncated cone of the same diameter. Volume of material removed was calculated from the geometry and hole depth for cylindrical and conical tools. Top surface of the workpiece was taken as the reference surface. The difference in Z-axis coordinate between the position of the tool tip at the bottom of the machined hole and the reference surface is measured as hole depth.

CHAPTER 4

RESULTS AND DISCUSSION

4.1. Introduction

This chapter discusses the results of the experiments conducted using the PCD tool in section 4.2. The results obtained for preliminary and main experiments using electroplated abrasive tools are discussed in sections 4.3 and 4.4 respectively. Section 4.5 discusses the mechanism of the material removal from the surface topography of the machined surface as seen in SEM images. Section 4.6 elaborates on the tool wear as a result of machining.

4.2. Results for Experiments with the PCD Tool

The effect of tool diameter, static load, abrasive size and spindle speed on the drilling speed are discussed in the following sections.

4.2.1. Effect of tool diameter

Figure 4.1 shows that a larger tool diameter leads to a higher material removal rate (MRR). Greater number of abrasive particles are available for material removal under the larger tool. Thus more cutting action takes place and results in higher MRR.

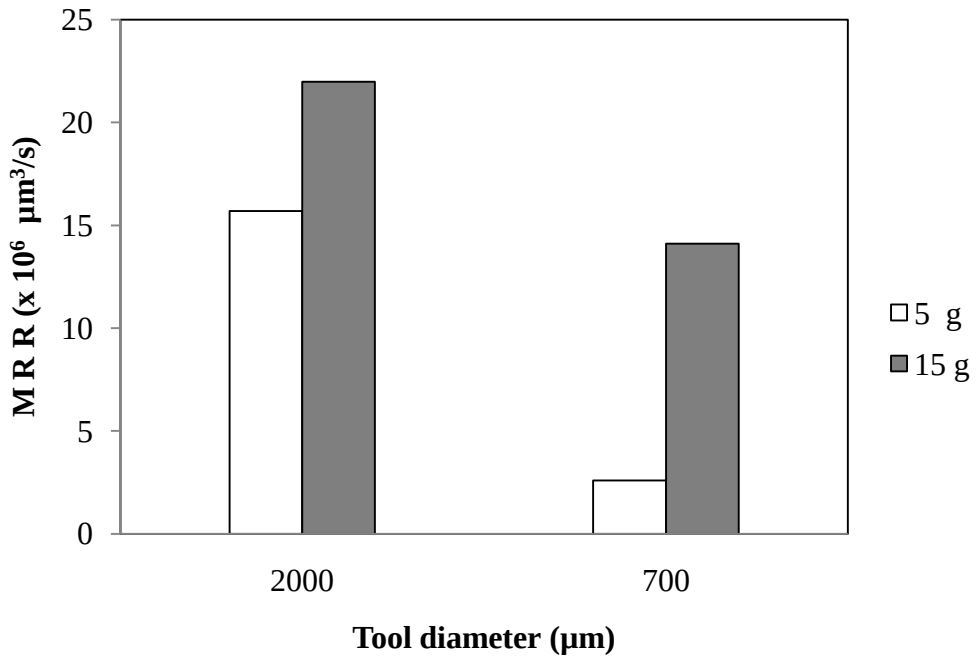

Figure 4.1. Effect of tool diameter on MRR *(machining time – 100 s, abrasive size – 3~5 µm)*

4.2.2. Effect of static load

For the given abrasive size and tool diameter, higher static load provides more contact pressure on the abrasive-workpiece interface and as a result more material is removed and deeper machining is achieved as shown in Figure 4.2.

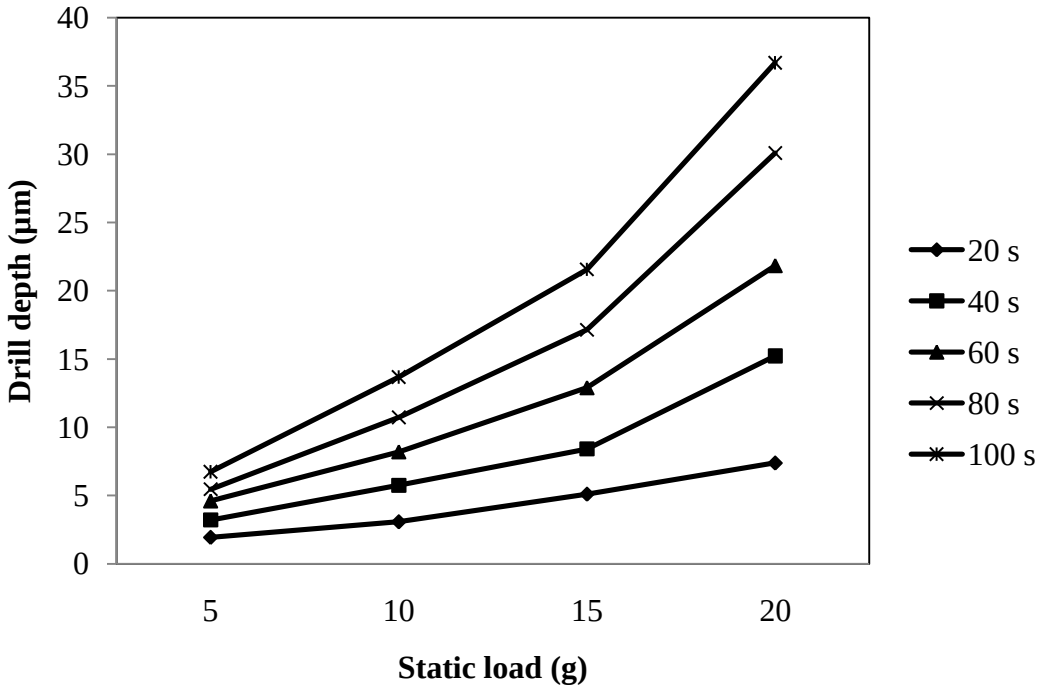

Figure 4.2. Effect of static load on drill depth

4.2.3. Effect of abrasive size

In general, for the given tool diameter, and abrasive particle size, larger abrasives provide greater machining. Depth achieved after 100 s of machining with a PCD tool (Diameter 700 µm) at static load of 20 g, abrasive particle size of 1~3 µm, 3~5 µm is shown in Figure 4.3.

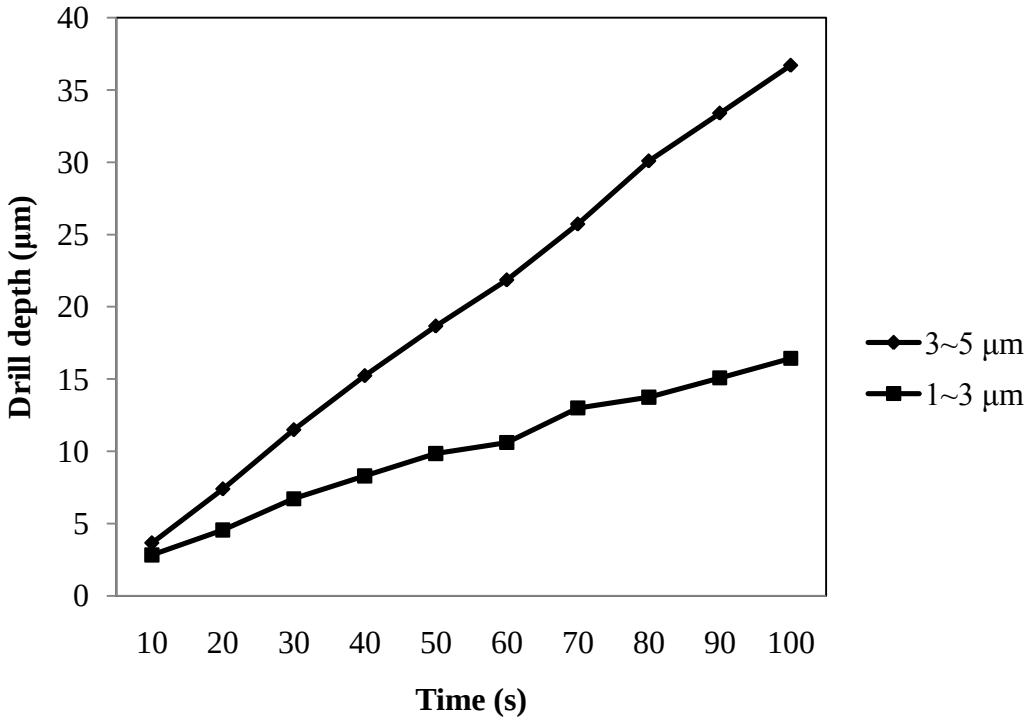

Figure 4.3. Effect of abrasive size on drill depth

4.2.4. Effect of spindle speed

The speed of tool rotation does not appear to have significant effect on the machining as shown in Figure 4.4. A tachometer was used in the experiments to check the speed of the spindle while machining. It was noticed that the spindle speed was not constant during the machining process. Along with the abrasive tool, abrasive slurry was also used for machining to achieve substantial machining.

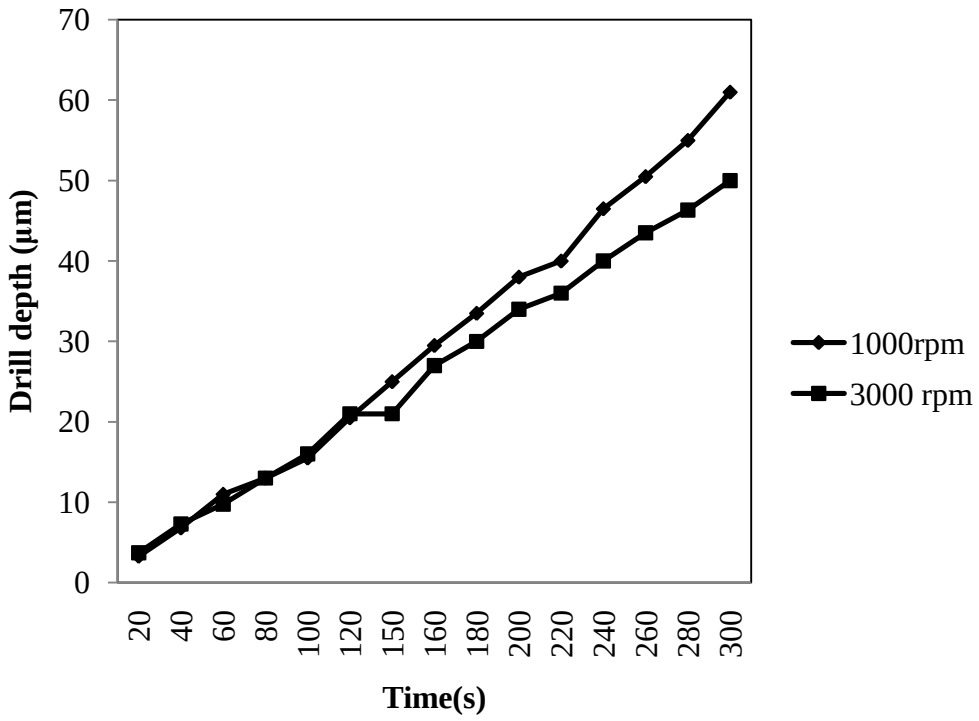

Figure 4.4. Effect of spindle speed on drill depth achieved by the PCD tool ***(tool diameter 500 µm, static load – 40 g, abrasive particle size – 1~3 µm)***

The contribution of the material removal due to the abrasive tool was dominated by the material removal due to the abrasive slurry. To facilitate machining by completely abandoning the abrasive slurry, electroplated abrasive tools with larger abrasives were used for the following experiments.

4.3. Results for Experiments using Electroplated Abrasive Tools

The effect of the static load, coolant, tool geometry on the material removal rate (MRR) is evaluated with the preliminary experiments to decide the appropriate levels of the parameters for the main experiments. The effect of spindle speed, grit size and vibration amplitude on the material removal rate is studied in the main experiments.

4.3.1. Effect of static load and coolant

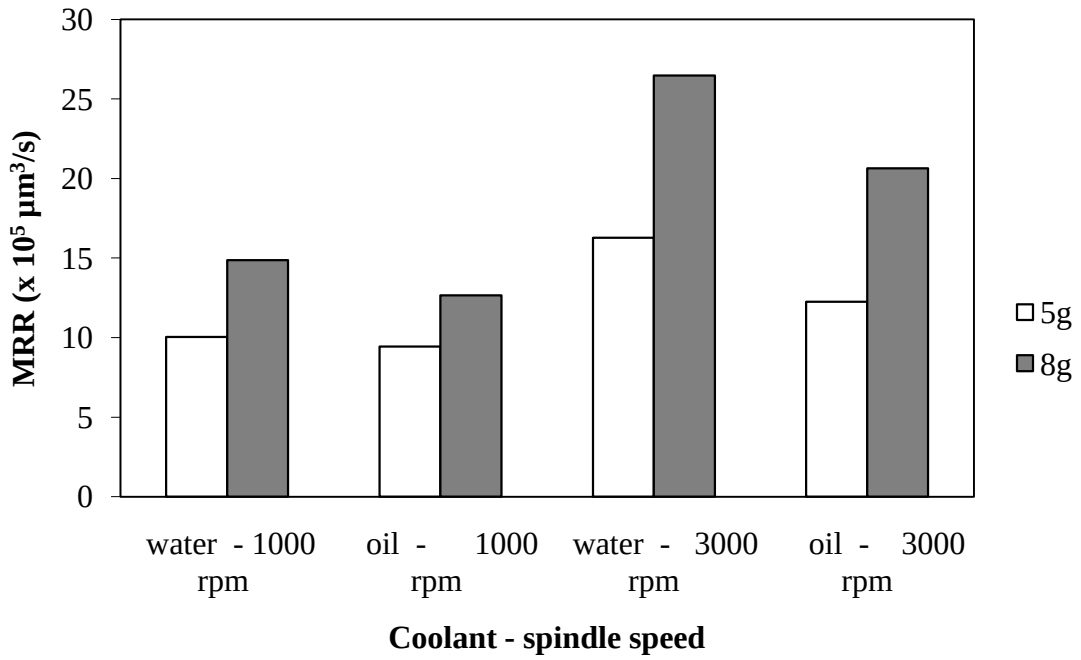

Figure 4.5. Effect of coolant, spindle speed, static load on MRR *(A = 1 µm, G = M, t = 200 seconds)*

MRR increased with the use of a higher static load at different spindle speeds as shown in Figure 4.5. The depth of indentation of each abrasive grit increased with increase in the static load. As a result the material removal rate was higher for the higher static load MRR was slightly higher when water was used as a coolant rather than oil. This difference was not obvious at the lower load and lower spindle speed. Even if the

use of different coolants did have an influence on the MRR, it was very small to draw any meaningful conclusions based on these experiments.

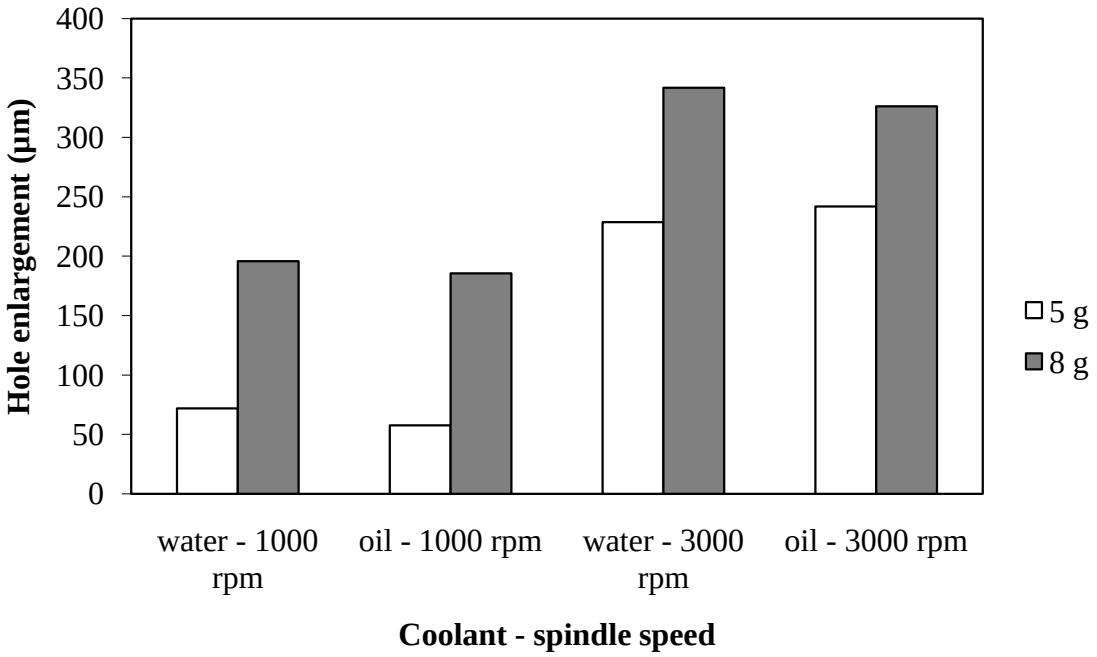

Figure 4.6. Effect of coolant, spindle speed and static load on hole enlargement *(A = 1 µm, G = M, t = 200 seconds)*

The static load and spindle speed were found to have an effect on the dimensional accuracy of the process as shown in Figure 4.6. Larger spindle speed and the higher static load applied resulted in a greater hole enlargement compared to a lower spindle speed and a lower static load. The hole enlargement was maximum when both spindle speed and static load were at the highest levels. On the other hand, hole enlargement was the lowest when both were at lower levels. At higher static load and spindle speeds the forces acting on the tool during machining are higher, thus leading to an increased swiveling of the tool on the workpiece.

With the help of the above discussion, a low static load of 5 g was chosen and oil was used as the coolant for all the experiments conducted for studying the effect of spindle speed, grit size, and vibration amplitude and tool shape.

4.3.2. Effect of tool shape on drill depth

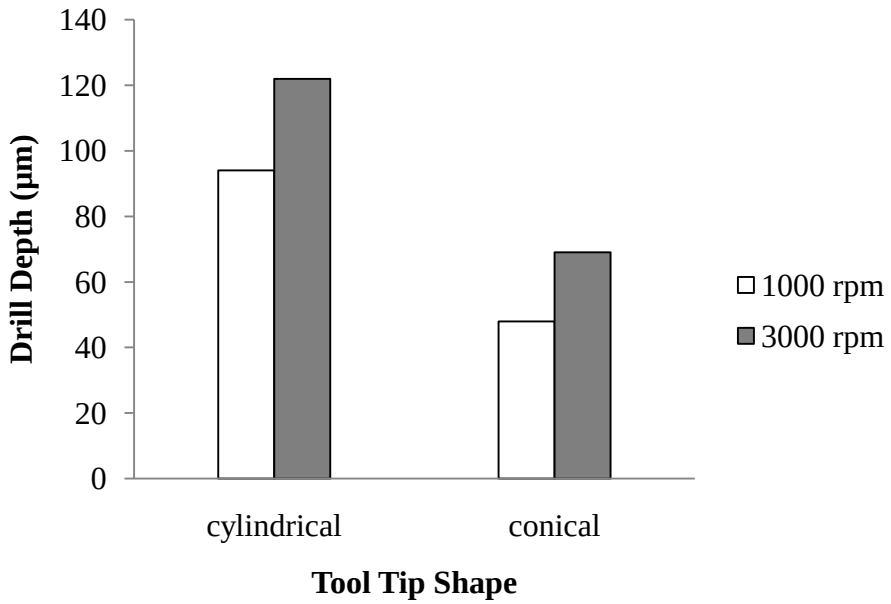

Figure 4.7. Effect of tool shape on drill depth ***(A = 1 µm, C = oil, G = M, SL = 5 g, t = 200 seconds)***

A comparison was made between the machining capability of a cylindrical tool and a conical tool as illustrated in Figure 4.7.

For different spindle speeds, the drilling depth achieved by the cylindrical tool was always higher than that for the conical tool. Since the tip of the cylindrical tool is larger than the conical tip, more number of abrasive grains could be bonded on the cylindrical tool tip. Thus the machining process was expedited when a cylindrical tool was used.

4.3.3. Effect of feedrate on the machining force

Machining experiments are usually performed by either keeping the feedrate constant or by keeping the force constant by controlling either parameter. Most of the reported literature on macro RUM uses constant feedrate mode of operation while for micro USM uses constant force (static load) mode. To decide the best choice for MRUM, MUSM setup was operated at constant feedrate mode.

All the previous experiments were conducted at constant force mode. To study the forces developed in MRUM, the tool was fed towards the workpiece at a constant feedrate. The force generated increased with increase in feedrate as shown in Figure 4.8. The highest average force was recorded for the highest feedrate. At the highest feedrate, the average force recorded was lowest for the highest speed of tool rotation used.

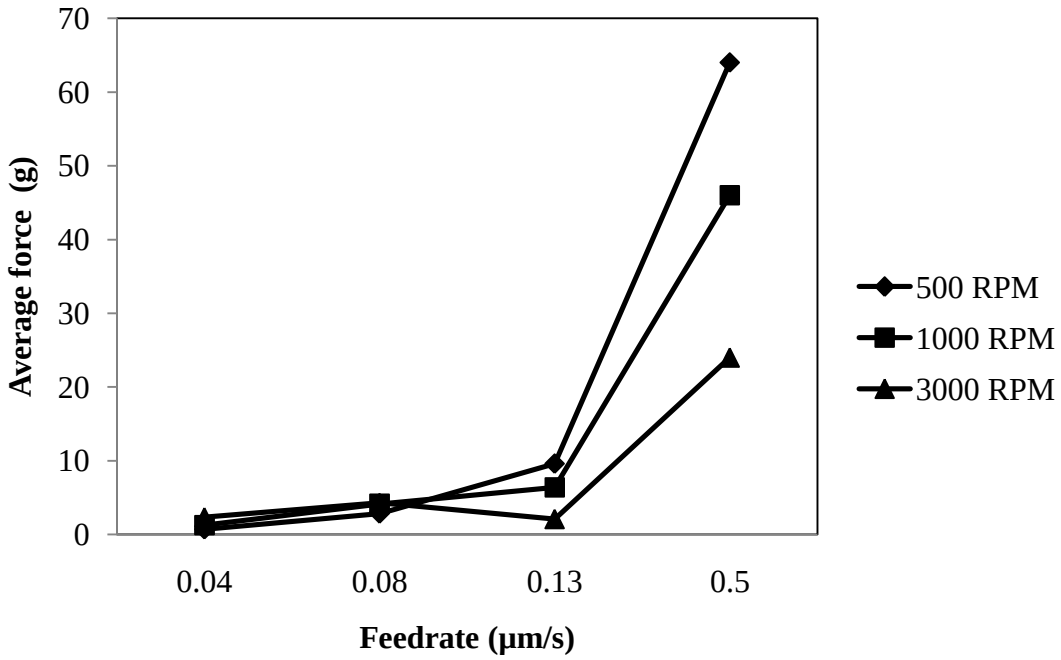

Figure 4.8. Effect of feedrate on the average machining force ***(A = 1 µm, C = oil, G = F, t = 400 seconds)***

The trend was not very clear for the lower feedrate values. While the force shows an increasing trend with increasing feedrate, the force value shoots up suddenly. This is because other factors such as stiffness of the machine also contribute to the recorded average force. Therefore, the average force does not give an accurate indication of the actual machining force developed at the contact interface of the tool and the workpiece. Inspite of this, the results do indicate that the machining forces developed are highest at lowest spindle speed and lowest at highest spindle speed. Also the machining force increases with increase in feedrate.

4.3.4. Effect of spindle speed and grit size on MRR

MRR increases with increase in spindle speed for all grit sizes and vibration amplitudes as illustrated in Figures 4.9 - 4.10. At a higher spindle speed, the contact length of an abrasive particle while sliding over the work surface is larger for the same period of time. Thus, the effective number of cutting edges of the abrasives coming in contact with the workpiece increases. Therefore, the material removal process is accelerated [58].

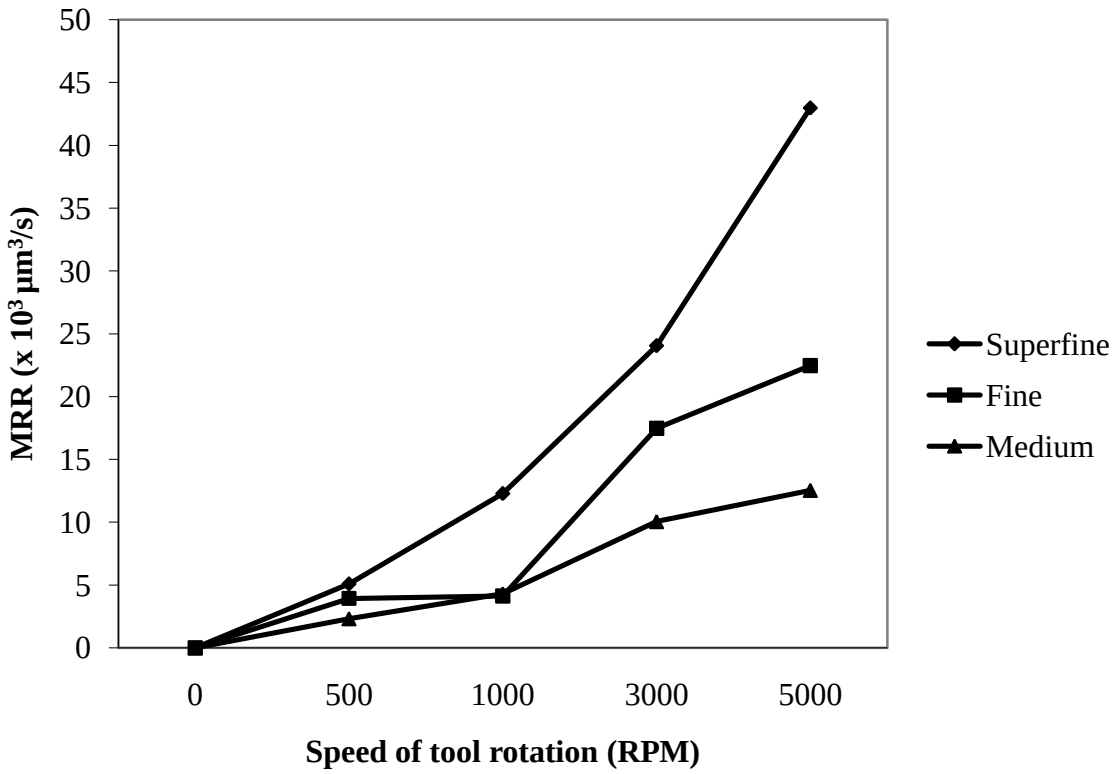

Figure 4.9. Effect of speed of tool rotation and grit size on MRR *(A = 1 µm, C = oil, SL = 5 g, t = 200 seconds)*

Another reason for the increase in MRR with spindle speed is the improved debris removal. At higher spindle speed, a higher centrifugal force facilitates the debris removal from the machining gap. The contribution of centrifugal force in removing the debris was evident when the machining was done without any coolant. The debris was found on the work surface surrounding the machined hole lying in a radial pattern.

For vibration amplitude of 1 µm, as shown in Figure 4.9, the grit size had an influence on the rate of the material removal. MRR was always the highest for the superfine grit size and lowest for the medium grit size at a given spindle speed. As the

spindle speed increased this difference in the MRR also increased and became clearer. Material removal process was enhanced the most by superfine grit size followed by fine and medium grit sizes, with increase in spindle speed.

For the vibration amplitude of 2.5 µm, the effect of grit size on MRR is insignificant, as shown in Figure 4.10. At a given spindle speed, MRR was almost the same for all grit sizes. The small variation could be attributed to the stochastic nature of the process arising due to several factors such as debris removal and nature (geometry and orientation) of the abrasive grits involved.

The use of larger abrasive size did not always lead to a higher MRR. This observation is consistent with that reported for machining using dental tool with different grit sizes [59]. In contrast, the MRR is observed to increase with increase in grit size for macro RUM [58]. In the experiments conducted, the size of the abrasive was almost comparable to the size of the tool tip. Thus, the tool essentially acted like a multipoint cutting tool. The increase of material removal rate was higher for the smaller grit size compared to the larger grit size when the spindle speed was increased from 0 to 5000 RPM.

Finally, the grit size was found to affect the MRR at the vibration amplitude of 1 µm but not at the amplitude of 2.5 µm. The material removal in RUM takes place because of the scratching action of the abrasive grains and microcracking caused due to the impact of the abrasive grains. At the lower vibration amplitude, MRR mainly takes place because of the abrasive grits scratching the work surface. Thus the size of the grain affects the MRR. At the higher vibration amplitude, the material removal due to

microcracking becomes more dominant. The size of the abrasive grain did not play a role in the material removal process.

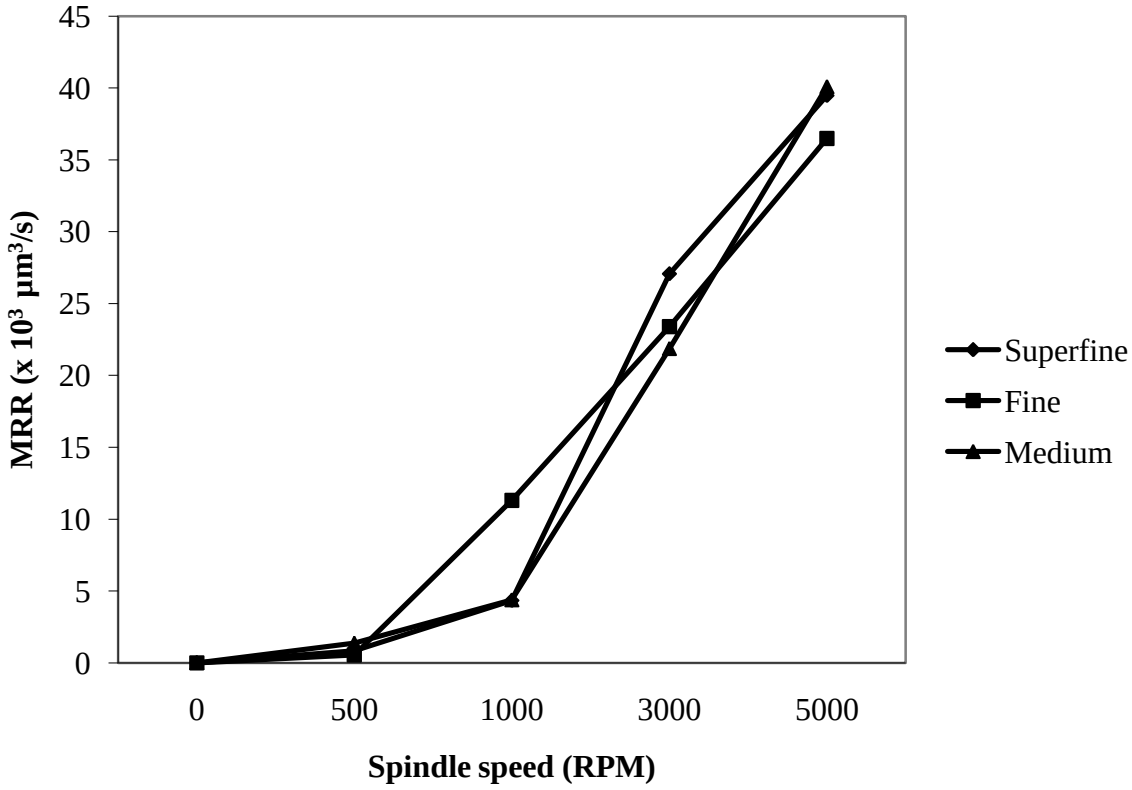

Figure 4.10. Effect of effect of speed of tool rotation and grit size on MRR ***(A = 2.5 µm, C = oil, SL = 5 g, t = 200 seconds)***

4.3.5. Effect of vibration amplitude on MRR

By increasing the drive voltage applied to the transducer, the vibration amplitude of the workpiece was increased. With increase in vibration amplitude the MRR also increased as shown in Figure 4.11.

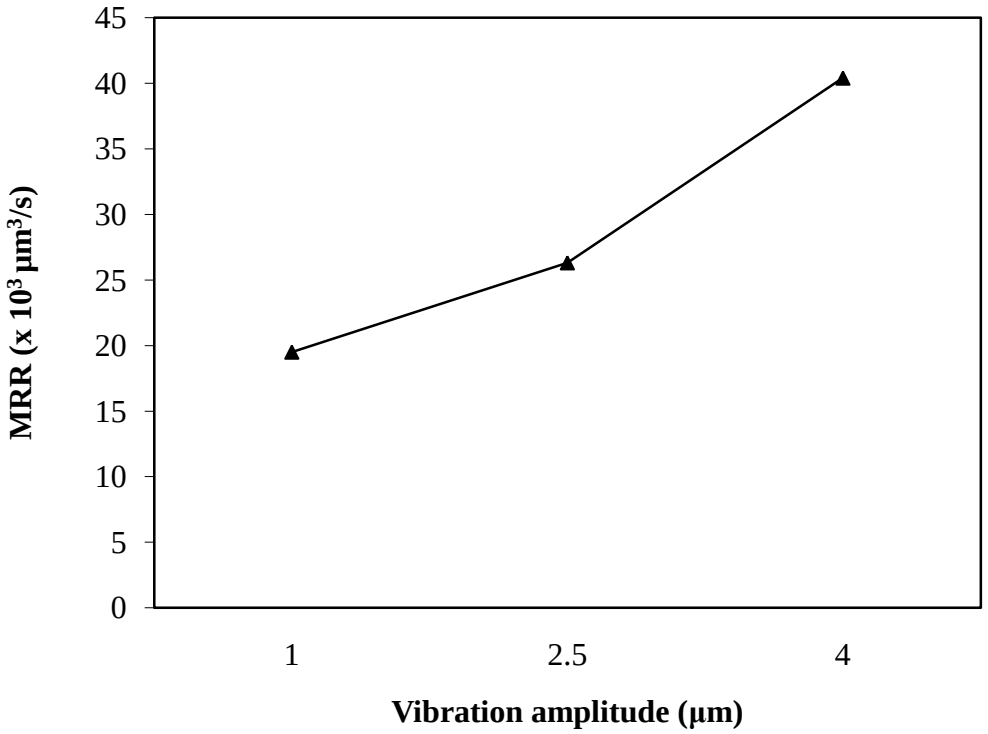

Figure 4.11. Effect of vibration amplitude on MRR *(C = oil, G = SF, S = 3000 RPM, SL = 5 g, t = 200 seconds)*

The impact, during machining with higher amplitude, was higher. Material removed by micro cracking was found to increase. The chipped material was removed during scratching by the abrasive grains due to tool rotation. For higher vibration amplitude, microcracking of the workpiece due to the repeated impact was a dominant mode of material removal, while for a lower amplitude, scratching of the workpiece was dominant.

With increase in the vibration amplitude, the gap distance present between the tool and the workpiece oscillated more. This led to an improved debris removal, thus aiding the MRR.

4.4. Mechanism of Material Removal

SEM images of the holes machined revealed evidence of both brittle fracture (brittle mode) and plastic flow (ductile mode) of material removal during machining. The scratch tracks of the abrasive grains on the machined surface could be seen clearly. Plowing was also observed along the sides of the track as illustrated in Figure 4.12. Although silicon workpiece was used which is brittle, there was evidence of ductile machining in the form of circular concentric grooves on the drilled surface in all the experiments. The number of these grooves was different for different experimental conditions, indicating the dependence of material removal by plastic flow on machining parameters. Figures 4.13 (a) illustrates machining with higher brittle machining while Figure 4.13 (b) illustrates a higher ductile machining contribution.

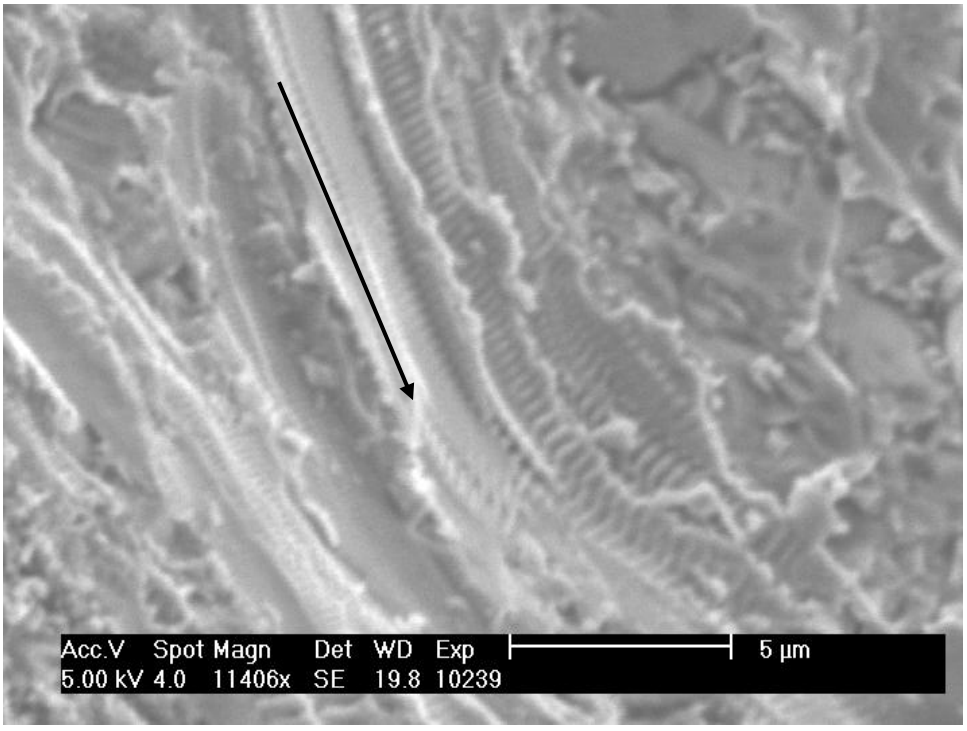

Figure 4.12. Scratch track of an abrasive grain on the silicon workpiece surface

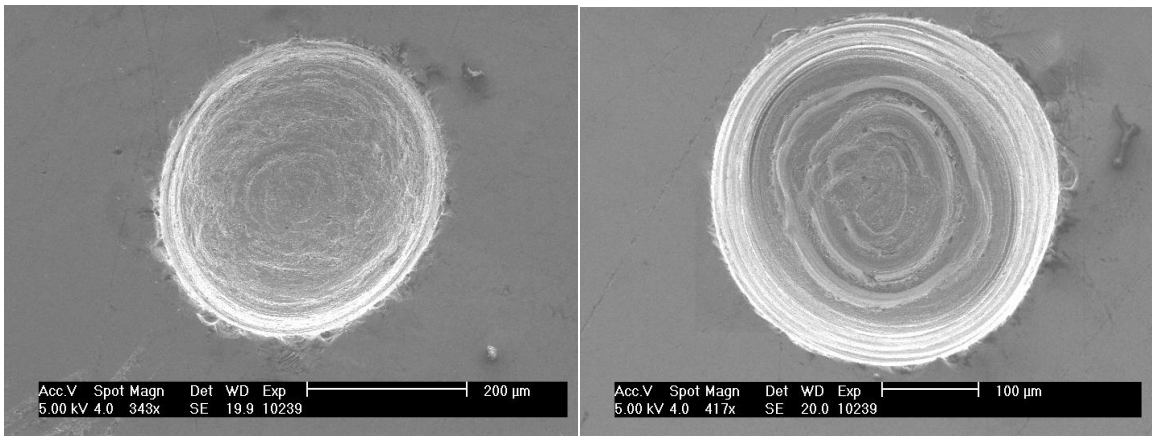

(a) (b)

Figure 4.13. Different contributions of brittle and ductile machining: (a) ductile machining is less evident (b) ductile machining is more evident because of the scratches present

Stick slip marks were noticed on the machined surface of silicon as shown in Figure 4.14. These marks were mostly present along the periphery of the hole in a concentric fashion. However, at few locations on the machined surface these marks were short and perpendicular to each other, indicating the participation of a number of grits as illustrated in Figure 4.15. These marks were also present on the diamond grain and surrounding metal matrix binding the abrasive grain as shown in Figures 4.16 - 4.17. Stick slip marks provide further evidence to the presence of ductile machining, however, it does not result in improved surface finish. Stiffness of the machine tool, tool eccentricity, and chattering might be the reasons for the stick slip phenomenon. Figure 4.18 illustrates small subsurface cracks beneath the machined surface. These cracks seem to be less than 2 µm deep.

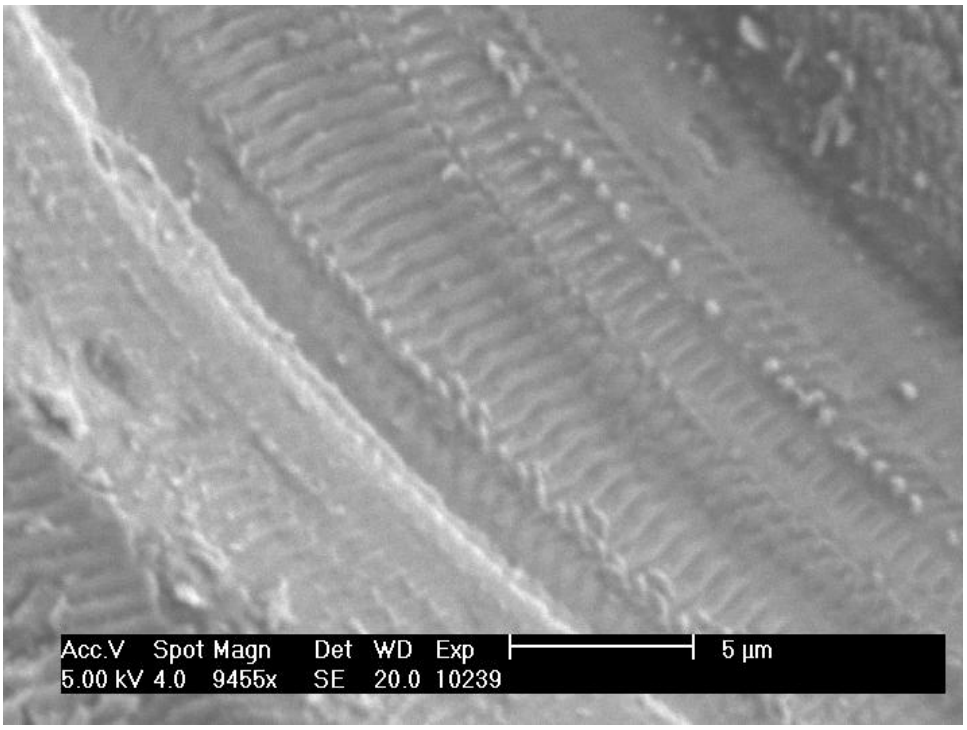

Figure 4.14. Stick slip marks on the machined surface of Si wafer

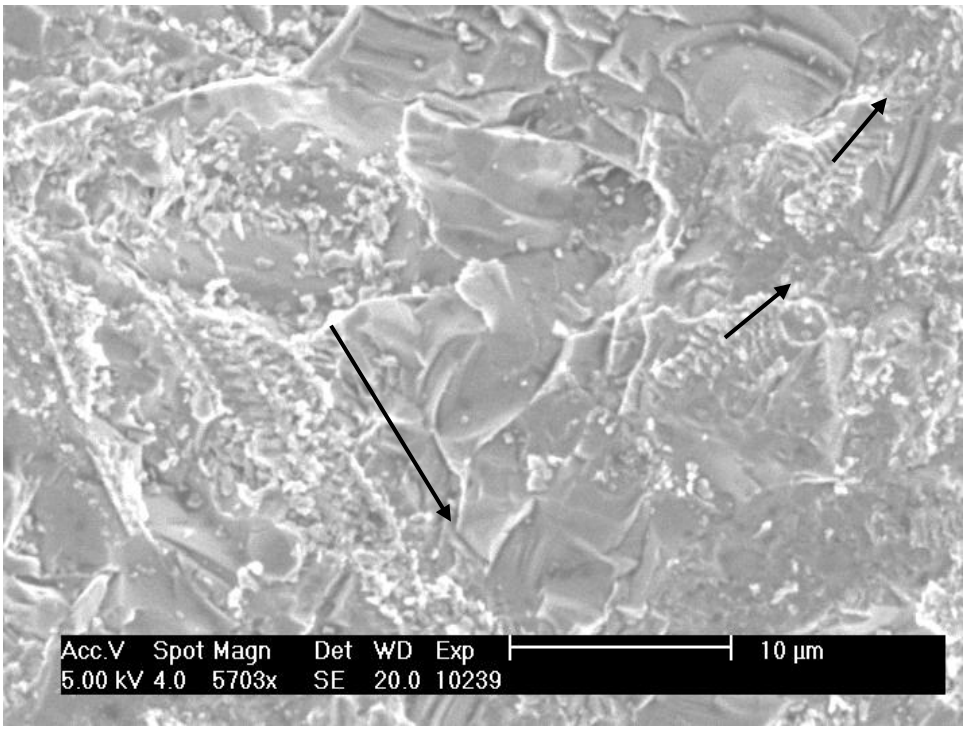

Figure 4.15. Perpendicular stick slip marks

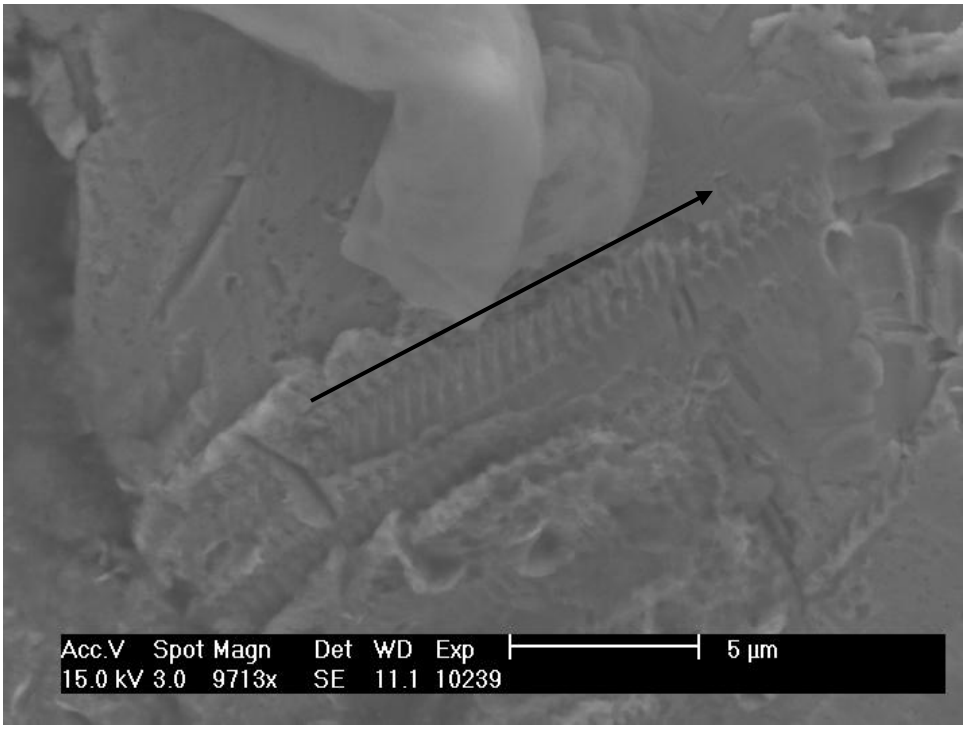

Figure 4.16. Wavy machining marks on the metal matrix of the tool

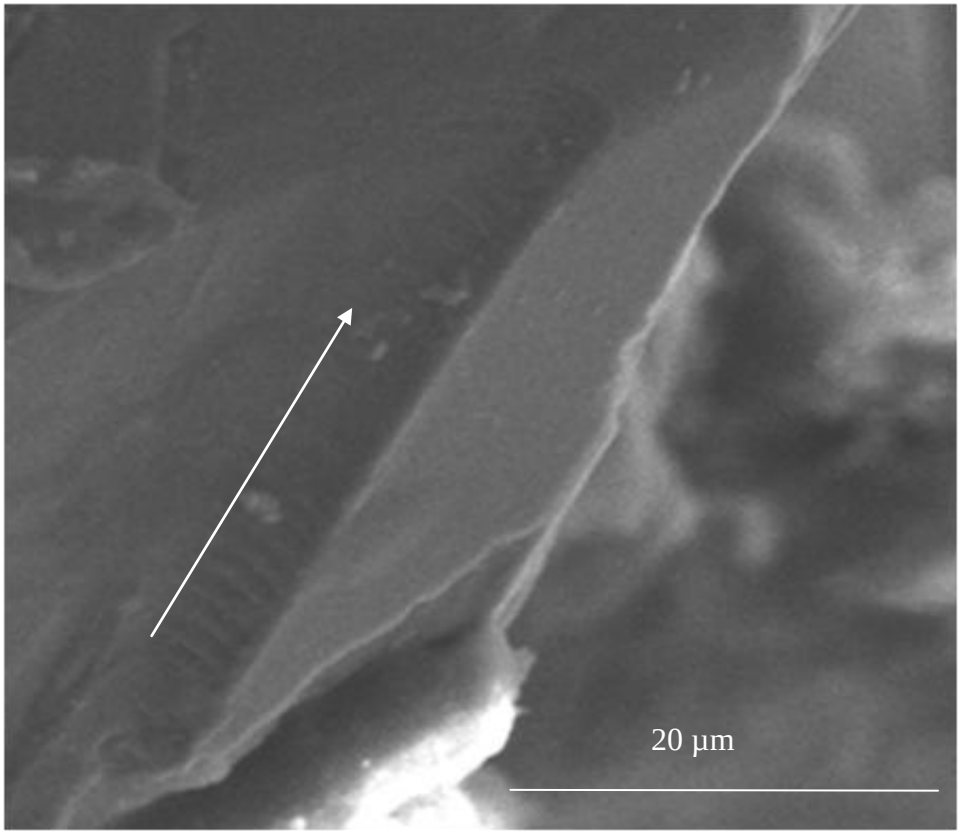

Figure 4.17. Wavy machining marks on the abrasive grain

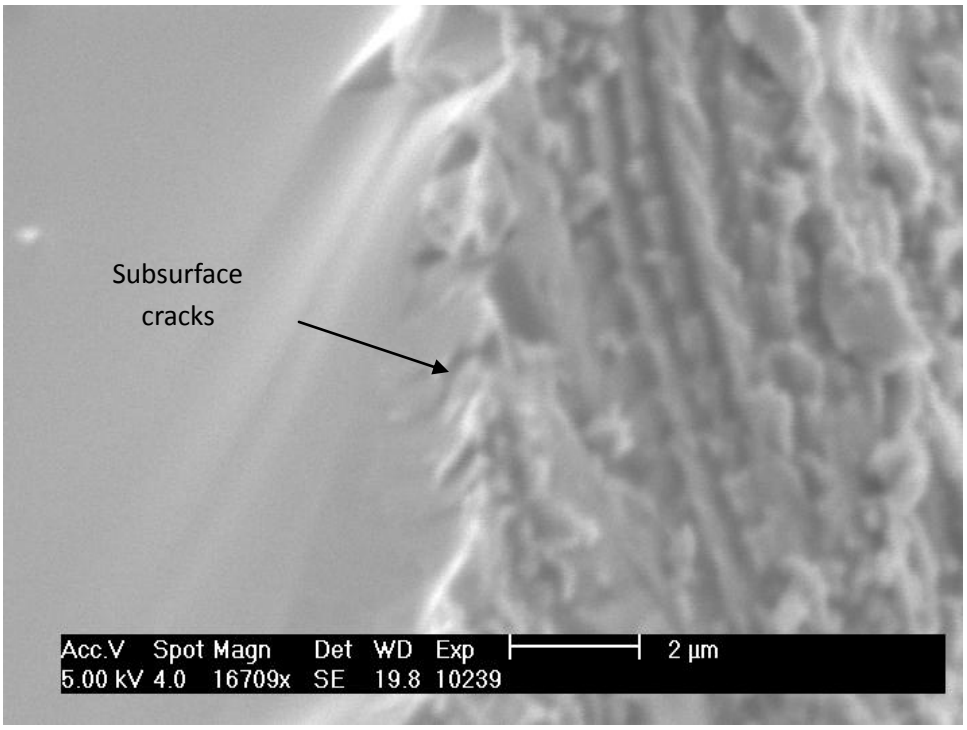

Figure 4.18. SEM image of silicon wafer showing subsurface damage after MRUM

4.5. Tool Wear

Tool wear was observed in the form of grain pullout as illustrated in Figure 4.19 and grain fracture as illustrated in Figure 4.20. Grain pullout was observed to occur often on the medium grit sized tool compared to the superfine and fine grits. The height of the protruding part of the grain was more for the medium grits, so the moment of force acting on the grit was more, thus making the medium grit more prone to pull out. In case of medium grit tool, fewer numbers of grits participate in the machining process. As a result the wear of medium grit tool was faster. Even though no abrasive slurry was present wear marks were observed on the tool. Figure 4.21 illustrates the wear marks on the metal matrix of the tool. The presence of the debris or pulled out abrasive grains in the machining gap could be a possible reason. Such an impact on the metal matrix might further increase the degree of tool wear.

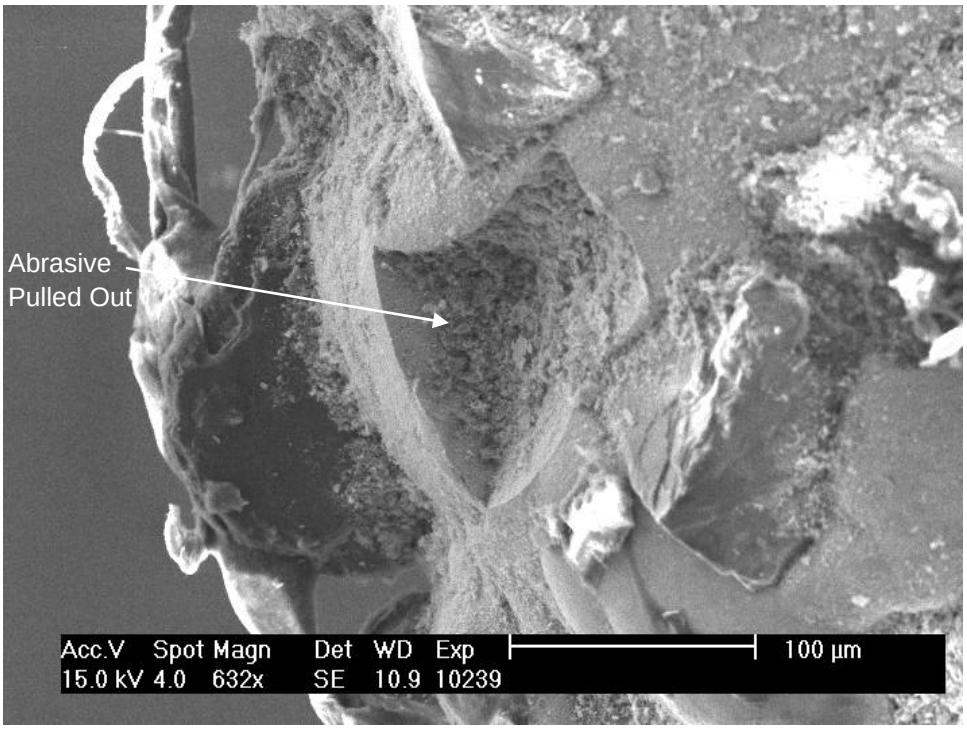

Figure 4.19. Cavity showing missing abrasive grain on the tool

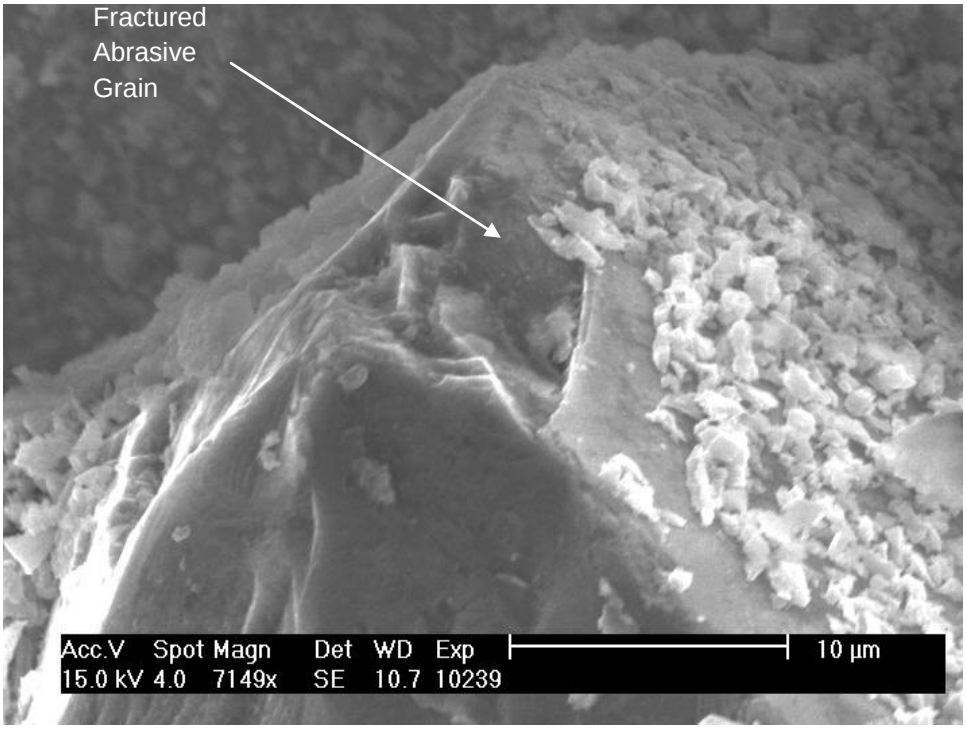

Figure 4.20. Fractured abrasive grain

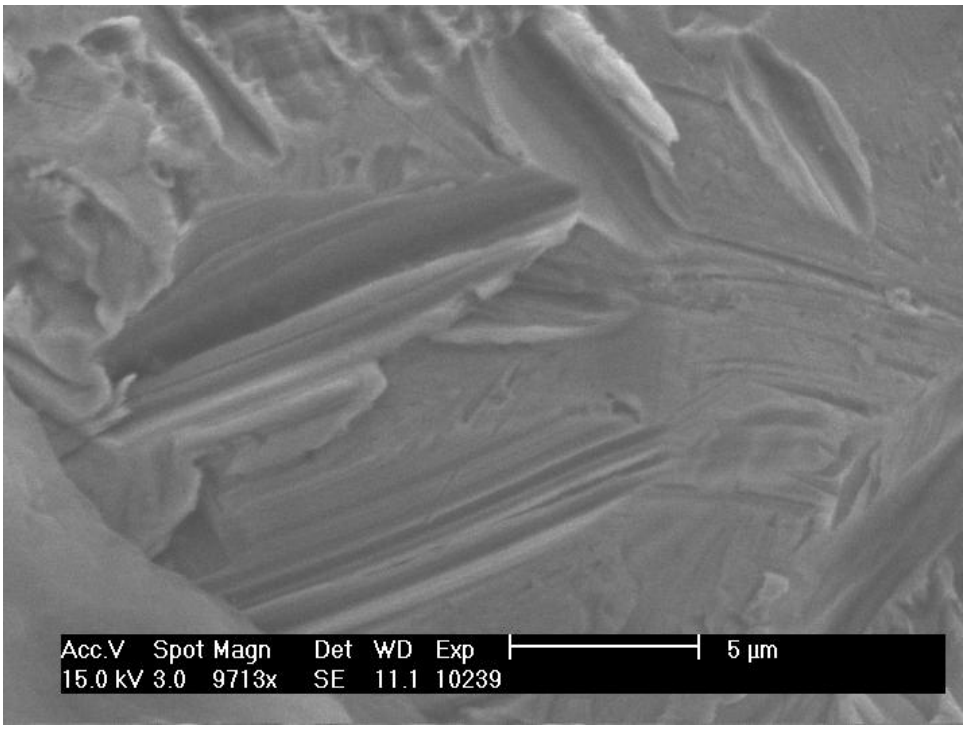

Figure 4.21. Wear marks on the metal matrix of the tool

CHAPTER 5

BONE MACHINING

5.1. Introduction

This chapter investigates machinability of bovine rib by using MRUM technique discussed in the previous chapters. Drilling micro holes into flat pieces of bovine rib was attempted. Experiments were performed under different spindle speeds and using different abrasive grit sizes. The material removal rate as a result was calculated from the drill depth achieved. The machined surface was studied under the scanning electron microscope (SEM) in an attempt to understand the mechanism of material removal. The edges of the drilled hole after machining were observed. Section 5.2 discusses the necessity for bone machining, the techniques used for bone machining and performance measures used for evaluating the techniques. Section 5.3 describes the experimental conditions and the workpiece preparation. Section 5.4 discusses the results obtained. The results are summarized in Section 5.5.

5.2. Literature Review for Bone Machining

5.2.1. The need and the issues in bone machining

Machining, cutting, drilling or finishing of bone - a hard tissue present in an animal body, is necessary for orthopedic and dental surgeries. Meso and micro scale machining of bone is necessary in applications such as stapedectomy (surgery of the ear bone (stapes)) [60, 61, 62], oral and maxillofacial surgeries [63], implantology [64], spinal surgery [65] and other minimally invasive surgeries. Accurate and precise machining is important in the above mentioned examples to avoid damage to the

neighboring tissues [63].

A critical issue during machining bone is the rise in temperature. High temperature (~50 ^{0}C) causes thermal damage to the bone cells (thermal necrosis) [66]. Since thermal conductivity of bone is low the heat generated in the working area is not dissipated easily. Therefore, increase in temperature during machining should be within the critical limit to avoid thermal necrosis. Exposure to high temperature also deteriorates the bone regeneration and healing. The occurrence of thermal necrosis also depends on the time for which the bone is exposed to the high temperature. If the duration of exposure to high temperature is small then even if the temperature is greater than the critical temperature, chances of thermal necrosis are reduced [67-72]. Machining by plastic deformation, though preferred for better accuracy, usually leads to increase in cutting temperature which increases the risk of thermal damage to the bone [73]. However ductile regime machining of brittle materials is desirable to minimize the subsurface damage [74]. It has been reported that in vibration assisted machining the use of ultrasonic vibrations reduces the stresses and the subsurface damage developed in the workpiece. As a result the strength of the workpiece after machining is maintained. The cutting forces developed are lower during vibration assisted machining compared to conventional grinding [56, 75]. In ultrasonic machining, the heat generated in the machining zone is not very high [76]. Evidence of ductile machining was observed during machining of silicon wafer using MRUM. Therefore it was hypothesized that it would be useful to explore the possibility of machining bone.

5.2.2. Techniques for bone machining

The reasons for machining bone during surgeries have been classified into the following three categories:

- ablating a pathological piece of bone whether or not followed by prosthetic replacement
- anatomical correction,
- removing a portion of bone that obstructs the main operation site and returning it to its original position at the end of the operation [67].

Depending on the operation, different techniques have been used for machining bone. Many clinical and non-clinical studies have been carried out for evaluating the performance of the machining techniques under different machining conditions. Table 5.1 presents the reported traditional and nontraditional machining techniques and their purpose.

Table 5.1. Techniques for machining bone

Traditional Techniques	**Purpose**
Drilling	Investigate the biocompatibility with implants [77], perforation [67]
Milling, HSM	Minimally invasive orthopedic surgery [78, 79], cortical bone reconstruction [80], surface preparation of bone [81]
Sawing	For cutting thick bones [67]
Coated cutting tools	Preparation of bone for biomedical implants, preparation of nanostructured surfaces [80]
Cutting method based on crack propagation	Machinining process for biomaterials, analysis of crack propagation in bone was used for cutting bone from the crack propagation characteristics [73]
Nontraditional Techniques	
Water jet cutting	Endoprosthesis revision surgery - removing prostheses rapidly with little damage to the surrounding tissue [83]
Abrasive water jet cutting	Endoprosthesis revision surgery [83] ; machining cancellous bone [84], cutting meat with bone [85]
Laser machining	Rotational Acetabular Osteotomy (RAO), to understand changes induced in bone in terms of temperature rise and thermal damage, feasibility of performing complete oesteotomy, examine bone healing under functional loading [86-89]
Ultrasonic osteotomy	To correct conditions of the jaw and face , to achieve a correct bite, an aesthetic face and an enlarged airway [90], sinus lift, alveolar ridge expansion, exposure of impacted canines, lateralization of the inferior alveolar nerve removal of osseous tissue close to the IAN, orthognathic surgery, autologous bone graft, harvesting, periodontal surgery, IAN transposition, alveolar distraction osteogenesis, and the removal of osseointegrated implants [64]
Non-invasive osteotomy	Use of focused ultrasound without incising the skin for ablating bone, for prospective surgical reconstruction of bone such as in RAO [91]

Typical performance measures of bone machining have been surface texture, surface integrity, and cutting force [92], temperature rise [93], bone healing after machining [77], efficiency, mechanical stresses developed, precision [73] and accuracy of machining.

The cortical bone is a one-direction, continuous fiber, reinforced-type of material

[73]. The structure of bone is very different from the other materials such as silicon machined by MRUM. So the influence of machining parameters was expected to be different.

For selecting an appropriate process for machining bone, it is important to understand its mechanical properties. Bone consists of a dense and hard outer tissue called cortical bone. Core of the bone is a porous and spongy tissue called cancellous bone. Cortical bone is anisotropic and is characterized by three different young's moduli, three different shear moduli and six Poisson's ratios. Depending on the species, age, anatomical site, liquid content etc, of the bone, the mechanical properties vary greatly [47]. Therefore, it is very difficult to specify accurate values of the material properties which play a role during machining. Moreover, bone is reported to have a hierarchical structure which means that it has different behavioral mechanics at macro, micro and nano levels [48]. Since the machining performance depends on the material properties of the tool and workpiece, knowledge of material properties of bone is important. The material properties for bovine cortical bone typically are the following: elastic modulus (GPa) 10–30, tensile strength (MPa) 70–150, elongation at fracture (%) 0–8, fracture toughness (MPa $m^{1/2}$) 2–8 [49].

5.3. Experimental Work

5.4.1. Workpiece preparation

A preserved bovine rib (1976) was cut into small flat pieces weighing 0.1g. The flat piece of cortical bone was obtained by grinding away cancellous bone and the curved portion of the cortical bone. Figure 5.1 shows a section of the bone exhibiting the spongy

cancellous inside and the hard cortical outside. The workpiece was mounted on the free end of the ultrasonic transducer and thus was vibrated ultrasonically.

(a) **(b)**

Figure 5.1. Pictures of the bovine rib (a) and its crossection (b) used as workpiece

5.4.2. Experiments

Experiments were performed under the machining conditions mentioned in Table 5.2.

Table 5.2. Experimental conditions for MRUM of bone

Parameters	**Levels**
Abrasive Grit Size	30, 50, 107~120 (μm)
Ultrasonic Vibration Amplitude	1 (μm)
Ultrasonic Vibration Frequency	39.5 (kHz)
Spindle Speed	0, 500, 1000, 3000, 5000 (RPM)
Static Load	5 (g)
Coolant	water
Tool Tip Shape	conical
Tool Feed Mode	force controlled mode
Machining Time	200 (seconds)

Five levels of spindle speeds (0, 500, 1000, 3000, 5000 RPM) and three levels of abrasive grit sizes (30 μm = Superfine (SF), 50 μm = Fine (F), 107~120 μm = Medium

(M)) were used for conducting the experiments. Each experiment was repeated three times and average material removal rate was recorded.

5.4. Results and Discussion

5.4.1. Effect of abrasive grit size and spindle speed on MRR

The material removal rate was found to increase with increase in the spindle speed and abrasive grit size as shown in Figure 5.2. As the speed of tool rotation increases the contact length of the abrasive grains sliding over the workpiece material during the same time increases. As a result more material is removed from the workpiece at a higher spindle speed [58]. This increasing trend in the result is similar to that reported for macro RUM of other materials [4, 5, 13] and MRUM of silicon as discussed in the Chapter 4.

At a given speed of tool rotation the MRR was found to be the highest for the medium sized grit and minimum for the superfine sized grit. While MRR for fine and superfine grit was close to each other for all the spindle speeds, it was much larger for medium grit. During machining of silicon wafer the material removal rate for superfine grit tool was found to be the highest followed by the fine and medium grit tools respectively as discussed in Chapter 5. This trend is opposite to that obtained during machining of bone. Because of the difference in the structural orientation and other mechanical properties such a change in trend was observed. Difference in the elastic properties of the bone and silicon might be responsible for this trend.

The bone is an anisotropic material. So the ease of machining depends on the direction in which the bone is machined. However, in the experiments conducted only circular holes were drilled. Therefore, direction of the fibers of the bone was immaterial.

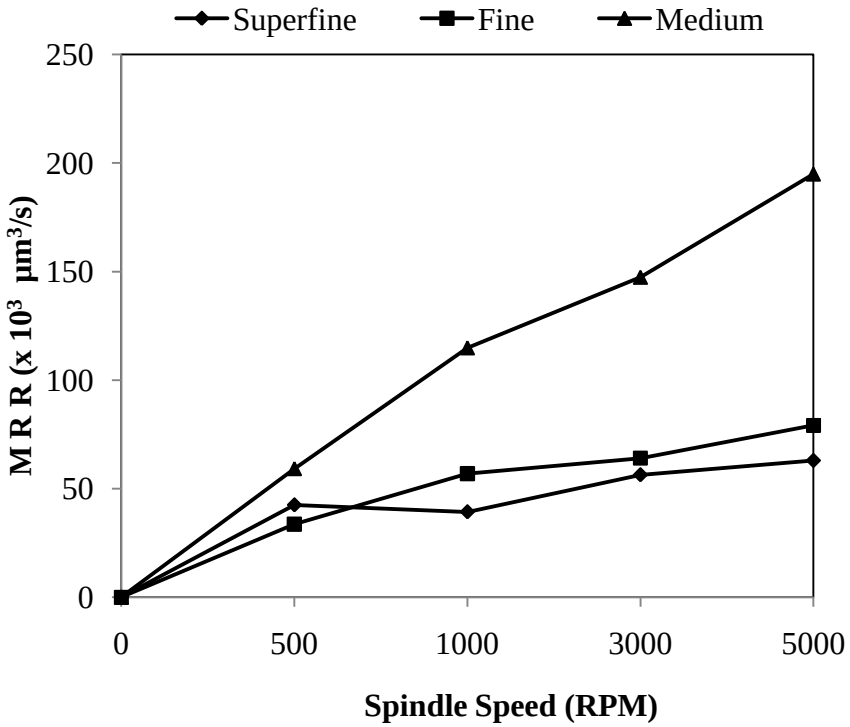

Figure 5.2: Effect of spindle speed and abrasive grit size on MRR

Under the same machining conditions when bone and silicon are machined, the MRR for bone is found to be much higher than silicon. Table 5.3 presents the material properties and MRR for bone and silicon. Evidently the material properties can be considered to be responsible for this difference in machining rate.

Table 5.3. Comparison of MRR for silicon and bone under same machining conditions

Workpiece	**Hardness** GPa	**Fracture toughness** MPa.m$^{1/2}$	**Modulous of elasticity (E)** GPa	**MRR** (x 10^3 µm^3/s)
Silicon	11.28	0.9	186	24.05
Bone	0.6-0.8	2–8	10–30	56.38

5.4.2. Quality of edge and hole circularity

The machined holes were circular and the edges of the holes were smooth. No prominent chipping was observed at the edges. Figure 5.3 illustrates a drilled hole. Figure 5.4 illustrates the surface topography of the drilled hole. Concentric scratch marks were observed on the surface.

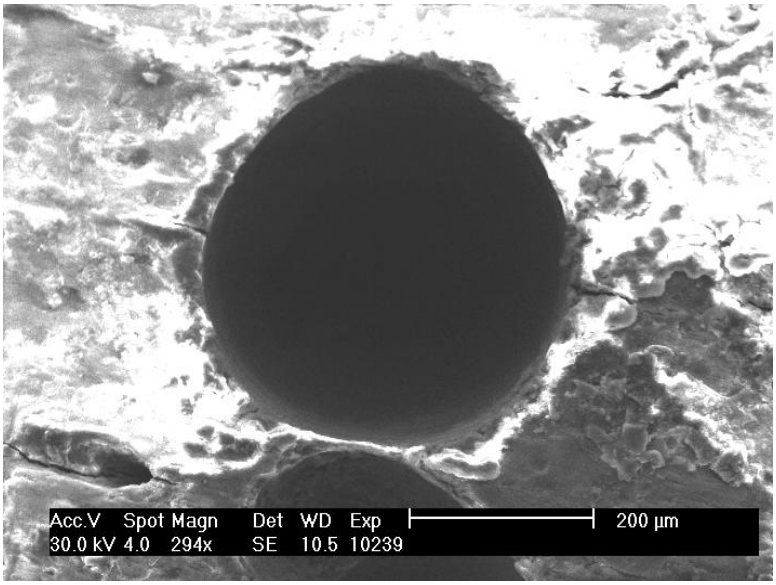

Figure 5.3: Circular machined hole with smooth edges

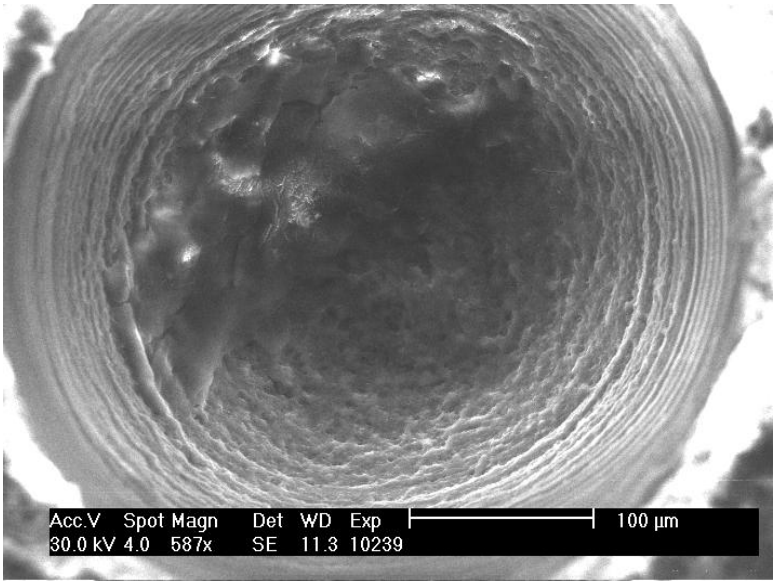

Figure 5.4. Surface topography of the drilled hole

Surface finish of the machined hole was not as smooth as the unmachined part of

the bone. Figures 5.5 and 5.6 illustrate the wavy machined wall of the hole and the smooth unmachined part of the bone. Use of smaller grit sizes might result in a better surface finish.

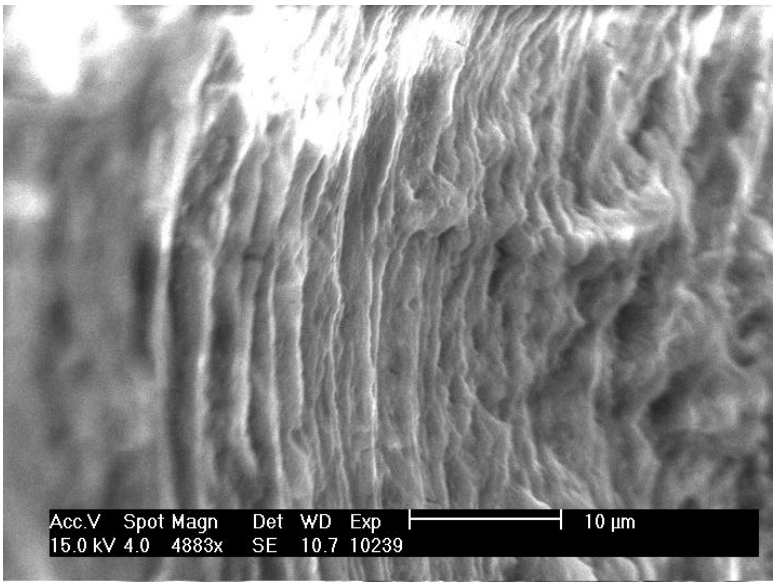

Figure 5.5. Wall of the machined hole

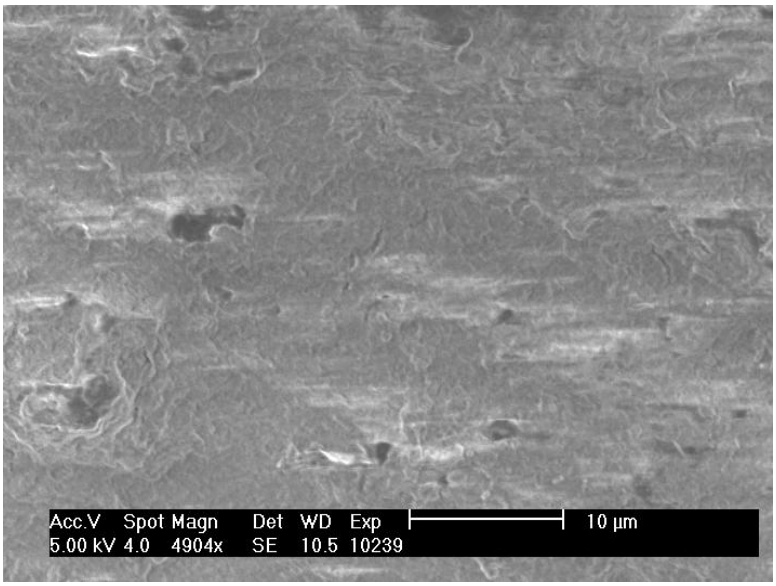

Figure 5.6. Unmachined surface of the bone

Therefore, to obtain an optimum machining performance, the mechanical properties of the workpiece must be considered. For preparing the bone surface for holding the implants, it is not always desirable to have a very smooth surface. A textured or a wrinkled surface offers more surface area for the cells to grow and attach to the implant. This enables better osseointegration (direct structural and functional connection between living bone and the surface of a load-bearing artificial implant, typically made of titanium). It is reported that the bone tissue can adapt to surface irregularities of 1-100 μm and that the surface stability can be greatly improved by introducing irregularities on the surface [50]. Instead of texturing the implant, texturing the bone is also proposed for enabling better osseointegration [51].

5.5. Summary

The study showed that Micro Rotary Ultrasonic Machining (MRUM) can be used for drilling holes in bone. The effect of change in abrasive grit sizes and spindle speed on the material removal rate was studied. Increase in spindle speed and grit size was found to increase the material removal rate (MRR). Quality of the edge of the machined hole, surface finish observed from the SEM images seemed reasonable.

CHAPTER 6

PREDICTIVE MODEL FOR MATERIAL REMOVAL RATE

6.1. Introduction

A literature review for various attempts made towards modeling of RUM is presented in Section 6.2. The physical description of the developed model for material removal by a single abrasive grain scratching and its extension to predict MRR in MRUM are presented in section 6.3. Section 6.4 describes the theoretical model for material removal by a single abrasive grain scratching and its modification for MRUM. Section 6.5 enlists the assumptions made during the development of the model. Section 6.6 presents the verification of the model and discussion.

6.2. Problem Description and Literature Review

Experimentation conducted in the previous chapters of this thesis yield information about the trends and parametric relationships for the material removal rate of MRUM. A mathematical model based on the process mechanism can predict the material removal rate without the need of actually performing the experiments. Rotary Ultrasonic Machining is a stochastic process because of the uncertainty arising due to factors such as the size, shape and the number of the abrasive grains participating in the material removal process, interference of the debris and tool wear. As a result it is difficult to incorporate the effect of all the parameters in the model for predicting the material removal rate. The actual problem can be simplified by making certain assumptions. Mathematical models developed for predicting the material removal rate rotary ultrasonic machining is presented in Table 6.1.

Table 6.1. Theoretical models for rotary ultrasonic machining

Models	Assumptions	Comments
Prabhakar, 1993 [50]	- Model for MRR - Workpiece material: Zirconia - Abrasive: Vickers indenter (modeled as spheres) - Working particles are of the same height - All working particles take part in cutting during each ultrasonic cycle - Volume of the material removed by one particle in one vibration cycle is equal to the intersection volume of the abrasive swept envelope and the workpiece.	- Crack formation by hammering action of ultrasonically vibrating tool considered to be major mode of MRR, plastic flow and scratching action was not considered - Modulus of Elasticity (E) and Poisson's ratio (ν) for abrasive along with workpiece are also accounted for
Pei, 1998 [16]	- Model for MRR - Workpiece material: Magnesia stabilized zirconia - Abrasive: Rigid spheres - Rest assumptions are same as those mentioned for Prabhakar (1993) model	- Numerical calculation of the volume of material removed by one particle within one vibration cycle was used, it was not calculated analytically - Model for material removal by plastic flow
Zhang, 2000 [6]	- Model for MRR - Workpiece material: Ceramics - Abrasive: Vickers indenter - Individual abrasive grain follows a linear path with constant depth of cut - Volume of the material removed is proportional to the dimensions of lateral crack and the length travelled by the abrasive under a constant normal load	- Model describes the effect of rotational speed in a limited way. Inefficient debris removal causes a decrease in MRR as the experiments suggest. This effect has not been modeled. - Higher loads result in the abrasive grain being in contact with the workpiece for a longer time. These effects are also not accounted for in the model.
Ya, 2002 [51]	- Model for MRR - Workpiece material: Glass - Workpiece modeled as Semi infinite solid - Abrasive: Rigid spheres - Maximum impacting depth in each vibration cycle is derived from Hertz theory	- Pressure distribution under each abrasive grain is considered - Distance of abrasive from the axis of the tool rotation is considered - Experimental verification of the model was not presented
Qin, 2009 [20]	- Model for cutting force - Workpiece material: Titanium alloy - Workpiece modeled as Rigid plastic - Abrasive: Rigid spheres - Rest assumptions are same as those mentioned for Prabhakar (1993) model	- Model for cutting force in a constant feedrate mode of operation - MRR is estimated from the feedrate - It is a physics-based models for RUM of metals

6.3. Physical Description of the Model

The mechanism of material removal due to the scratching action of the abrasive grain is reported to be mainly because of the lateral cracks in brittle material materials such as ceramics [94]. The mechanism of the material removal is illustrated in Figure 6.1. As the normal force P_n increases, the workpiece surface deforms plastically. When the normal force exceeds a threshold force lateral cracking occurs. The extent of lateral cracking is responsible for the material removal rate. The plastic flow during surface penetration increases the thermal stresses thus aiding the extension of lateral cracks [94].

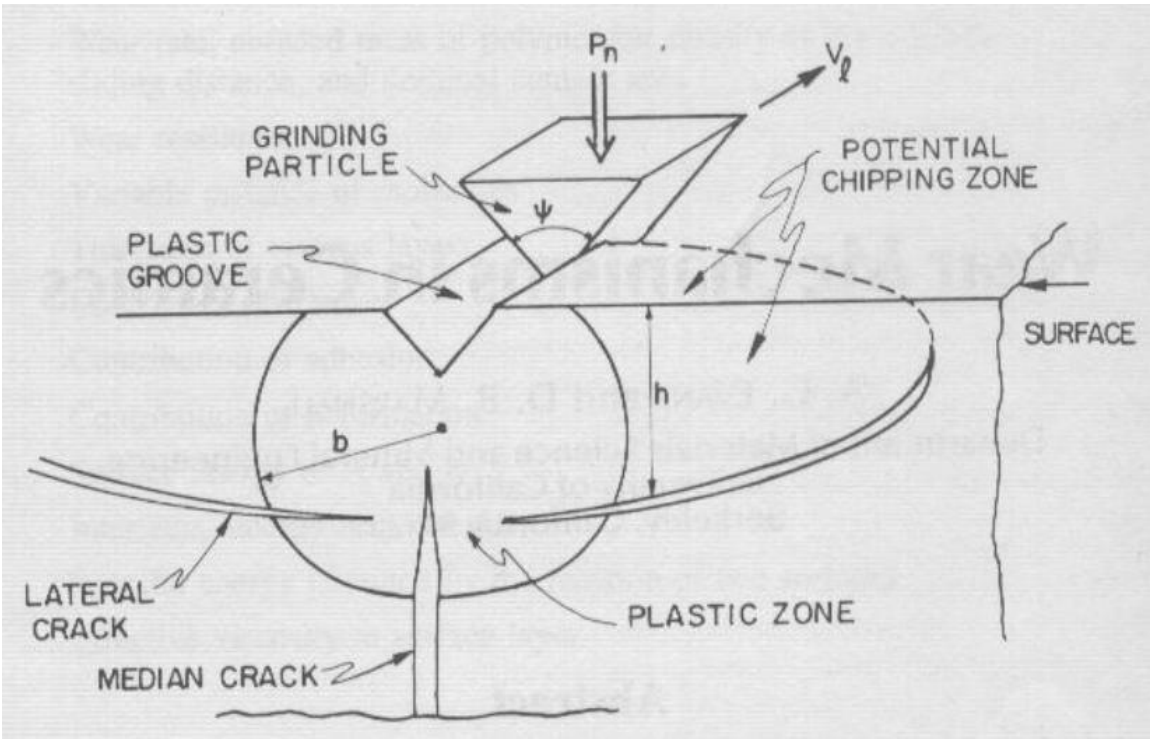

Figure 6.1. Material removal by lateral fracture mechanism [94]

The volume of the material removed by an abrasive grain is reported to depend on the material hardness (H_v), toughness (K_c), the normal force ($P_{n)}$ and the length (l) for which the abrasive grain travels on the workpiece with a constant depth of cut [94]. However, RUM is a hybrid process between grinding and ultrasonic machining. Therefore, along with the grinding action of the abrasive, material is also removed because of the impact action of the abrasive. As a result, the normal force on the abrasive grain oscillates ultrasonically with the frequency of the ultrasonic vibrations applied to the workpiece. Consequently, the force is more than the normal force alone which is assumed in grinding. Moreover, because of the vibrations, the contact between the abrasive grains and the workpiece are not continuous. Therefore, the length of travel of the abrasive grain on the workpiece is not continuous as illustrated in Figure 6.2.

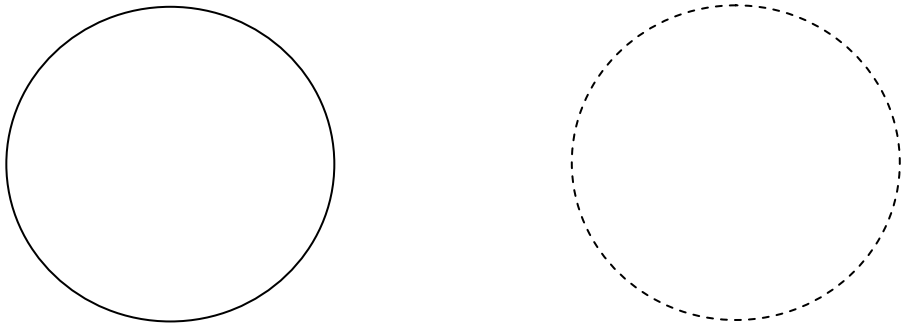

(a) **(b)**

Figure 6.2. Contact path of a single abrasive on the tool without ultrasonic vibrations (a) and with ultrasonic vibrations (b)

To befit the model of grinding action of the abrasive to RUM, the effect of ultrasonically oscillating force and the actual length of contact between the abrasive and the tool are considered.

6.4. Basic Assumptions for the Model

1. The workpiece is a brittle material.
2. The tool tip is cylindrical in shape. Since the radius of the tool is very small, the abrasive grains are assumed to be situated at the distance equal to the radius from the axis of the tool rotation. The abrasive grains are rigid sharp indenters as shown in the Figure 6.1.
3. The protruding height of the abrasive grains is assumed to be uniform.
4. The tool (abrasive grains) and the workpiece are in contact with each other only during certain portion of the ultrasonic vibration cycle. Therefore, machining is assumed to take place by grinding action during this contact time while machining due to abrasive impact occurs when the abrasive grain is indented onto the workpiece during each vibration cycle. For the purpose of verification the contact time between the abrasive grain and the workpiece is assumed to be 30% of the vibration cycle.
5. The frequency of the oscillations of the ultrasonic transducer is very high compared to the response time of the feedback system controlling the tool position. Therefore, the tool is assumed to be stationary and only the workpiece is assumed to vibrate ultrasonically.

6. The equivalent mass of the tool-ultrasonic transducer assembly is assumed to be equal to the mass of the ultrasonic transducer because it is the only vibrating part in the system.
7. Lateral cracking of the workpiece under the effect of an abrasive indenter is assumed to be the main reason for the material removal.
8. Material properties of the workpiece are assumed to remain unchanged during the machining process thus ignoring other effects such as the strain hardening effect and thermal effects.
9. Tool wear is not significant to affect the material removal rate.
10. The equivalent mass of the vibrating system is assumed to be 1/3rd of the mass of the transducer [95].

6.5. Development of the Model

It is proposed that in MRUM, fracture occurs during impact and fragmentation is completed due to plowing action during the contact period of abrasive particle and the work surface. Lateral Fracture Model [94] is used for predicting material removed by single abrasive grain when it slides over a brittle material for a distance *l*. Theoretically,

$$Volume\ of\ the\ material\ removed = 2 * h * c * l \tag{6.1}$$

where c is the extent and h is the depth of the lateral crack.

The volume of the material removed by single abrasive grain can be expressed as Equation 6.2 as given in the wear of ceramics [94].

$$Volume\ of\ material\ removed = \alpha_l * \left[\frac{P^{9/8}}{H^{5/8}K_c^{1/2}}\right] * \left[\frac{E}{H}\right]^{4/5} * l \quad (6.2)$$

where

α_l = material-independent constant

P = peak normal force

H = Vickers hardness

K_c = toughness

E = modulus of elasticity

To modify this model to predict the MRR for MRUM, the impact action of the abrasive grains and the intermittent contact length are considered.

To account for the impact action of the abrasive grains as they penetrate the workpiece during each vibration cycle, the normal force must be assumed to be dynamic. The state of vibration of the workpiece can be expressed as

$$y(t) = Asin(2\pi ft) \quad (6.3)$$

where

y(t) is the displacement of the workpiece, A and f are the amplitude and frequency of ultrasonic vibrations applied to the workpiece.

The dynamic impacting force is given by

$$F_t = \frac{M}{\Delta T}y'(t) = \frac{M}{\Delta T}2\pi fAcos(2\pi ft) \quad (6.4)$$

where M is the equivalent mass of the vibrating system including the tool and the transducer, ΔT is the time for which the tool is in contact with the workpiece during each vibration cycle.

Thus during machining, the effective force acting on the workpiece is due to both the dynamic force (F_t) and the static force (W) [6].

$$F = W + F_t = W + \frac{M}{\Delta T} 2\pi f A cos(2\pi f t) \tag{6.5}$$

The maximum impact force acting on a single abrasive grain can be given by Equation 6.6. [6]

$$P = \frac{F_{max}}{N} = \frac{1}{N}(W + \frac{2\pi f A M}{\Delta T}) \tag{6.6}$$

where N is the number of effective abrasive grains participating in the machining process at a given time. Theoretically, N can be calculated by Equation 6.7. [6]

$$N = \frac{\pi r^2}{d_o^2}(\frac{6v_g}{\pi})^{2/3} \tag{6.7}$$

where

v_g= concentration of abrasive grains

d_o = mean diameter of the grains

The abrasive grain concentration v_g is assumed to be 100% for verification purposes.

The abrasive grain comes in contact with the workpiece intermittently because of the ultrasonic vibrations. Therefore, the length of travel of the abrasive grain over the workpiece needs to be calculated.

The number of impacts in one rotation of the spindle speed can be given by

$$Number\ of\ impacts\ in\ one\ tool\ rotation, I = f \times \frac{60}{RPM} \tag{6.8}$$

In each vibration cycle the abrasive grain is in contact with the workpiece for only a fraction of time which is less than 50% of the cycle time. Figure 6.3 illustrates one vibration cycle. During the cycle, the abrasive grain is in contact with the workpiece for time ΔT (t_1-t_0).

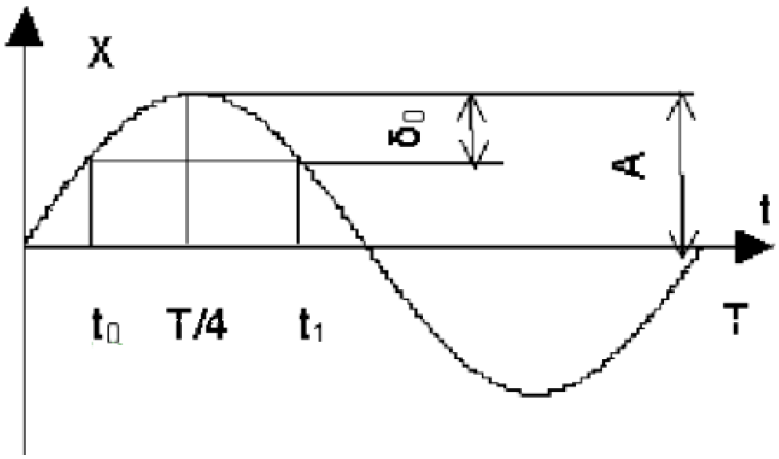

Figure 6.3. Contact time of the abrasive grain in one vibration cycle

Thus, the actual contact length of an abrasive grain during a single impact is given by Equation 6.9.

$$l = \frac{2\pi r}{I} \times \Delta T \times f \tag{6.9}$$

where t_c is the percentage of time period of the contact cycle for which the abrasive grain is in contact with the workpiece.

Therefore, after substituting the expressions for the ultrasonic impact force (Equation 6.6) and the length of travel of the abrasive grain (Equation 6.9) in Equation 6.2, the volume of the material removed by one abrasive grain in one contact cycle is given by Equation 6.10.

$$Va = \alpha_l \left[\frac{[\frac{1}{N}(W + \frac{2\pi f A M}{\Delta T})]^{9/8}}{H^{5/8} K_c^{1/2}} \right] [\frac{E}{H}]^{4/5} [\frac{2\pi r}{I} \times \Delta T \times f] \tag{6.10}$$

Finally the volume of material removed can be given by the expression in Equation 6.11.

$$V = Va \times I \times \frac{S}{60} \times N$$

$$V = \alpha_l \left[\frac{[\frac{1}{N}(W + \frac{2\pi f A M}{\Delta T})]^{9/8}}{H^{5/8} K_c^{1/2}} \right] [\frac{E}{H}]^{4/5} [2\pi r \times \Delta T \times f \times \frac{S}{60} \times N] \tag{6.11}$$

6.6. Model Verification and Discussion

In this section the results of the model were compared with the experimental data. Table 6.2 presents the machining conditions and the material properties. The model was verified for different spindle speeds and grit sizes.

The value of α_l was calculated from a set of experiments performed under vibration amplitude of 1 µm and spindle speed of 3000 RPM. The rest of the machining conditions are mentioned in Table 6.2. The value of α_l was found to be 9.179×10^{-9}. Figure 6.4 shows the comparison of results of the model with the experimental results.

Table 6.2. Machining conditions and material properties

Vibration Frequency	39.5 (kHz)
Vibration Amplitude	2.5 (µm)
Abrasive Particle Material	Polycrystalline diamond
Abrasive Particle Diameter, d_0	30, 50, 107~120 (µm)
Workpiece Material	Silicon <1 1 1>
Toughness, K_c	0.9 ($MPa.m^{1/2}$)
Vickers Hardness, H_v	1015 (kgf/mm^2)
Elastic Modulus, E	186 (GPa)
Equivalent Vibrating Mass, M	30 (g)
Spindle Speed, S	500, 1000, 3000, 5000 (RPM)
Tool Diameter	200 (µm)
Static Load, W	5 (g)

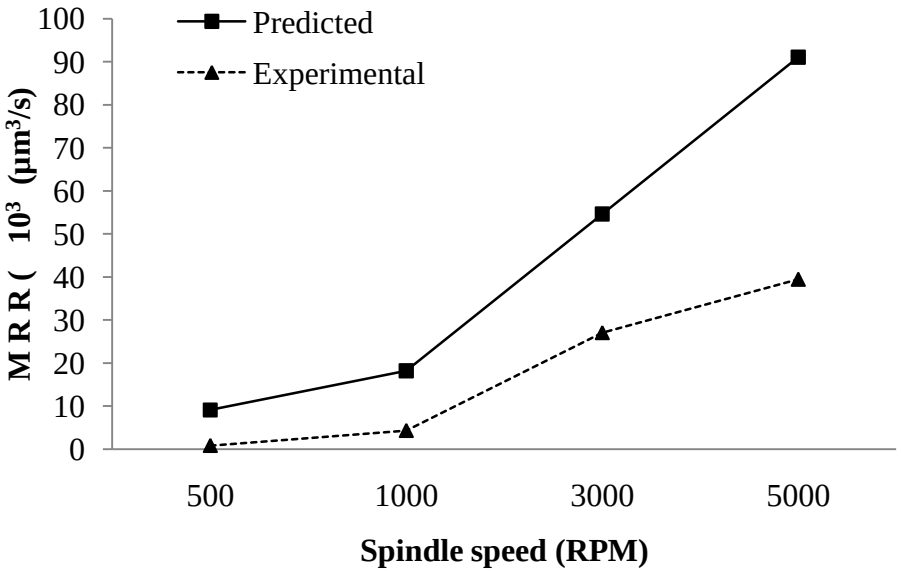

(a)

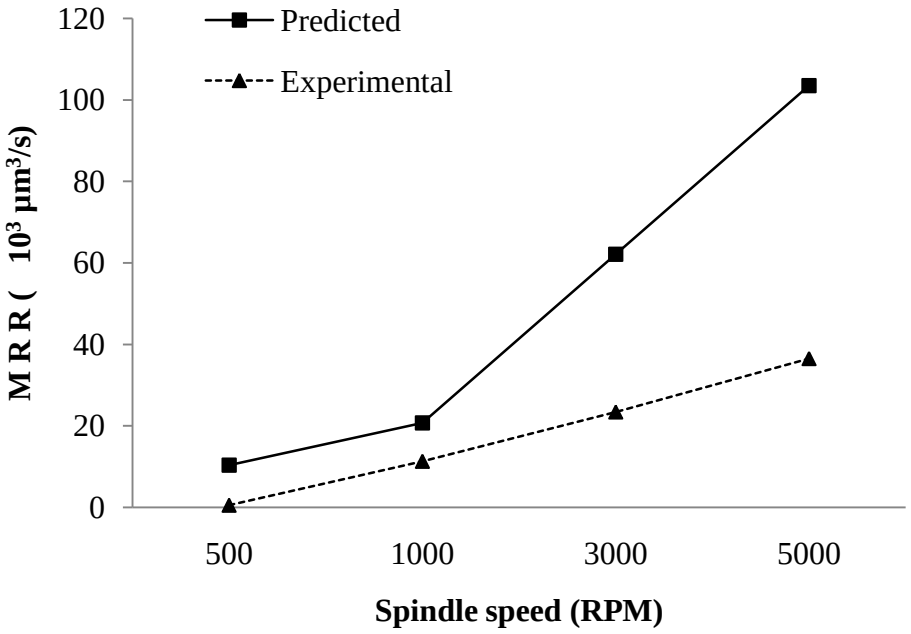

(b)

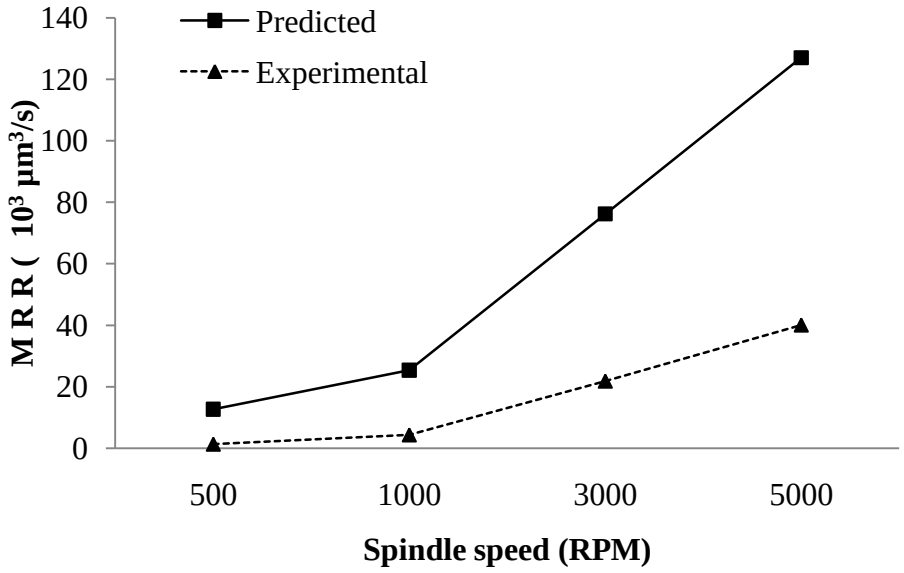

(c)

Figure 6.4. Plot showing experimental and predicted MRR for grit sizes 30 µm (a), 50 µm (b) and 107~120 µm (c)

The model overestimates the MRR for all the experimental conditions considered. The prediction is closer to the experimental value at lower spindle speeds. However, this difference becomes larger as the spindle speed increases. The model assumes that material is removed by each abrasive grain in every contact cycle. However, during actual experimentation this is not possible. The tool wears during machining leading to loss of abrasives grains. Therefore, MRR does not increase as fast as predicted with the increase in spindle speed.

The model assumes that the indentation forces are sufficiently in excess of the threshold force responsible for generating cracks. Only when the indentation forces are sufficiently large, the estimation of the length of the lateral crack (c) holds [94]. However, during experiments, this cannot be guaranteed because of the non-uniform height of the protruding abrasive grains and the hemispherical shape of the tool tip. Intermediate forces present may produce lesser and shorter cracks. Thus, the model provides an upper bound for the material removal.

In an attempt to maintain a constant static force, the tool moves up and down depending on the feedback. However, the response of the tool is not fast enough to change instantly with the changing forces. This may result in undesirable noncontact time. The model does not consider this possibility.

6.7. Limitations of the Model

The model is generally limited because of the assumptions made. This model does not consider the effect of tool wear, interference of the debris, probability of the abrasive

grains participating in machining process. The value of the material independent constant α_l depends on the experiments previously conducted on the same system. The material removal by plastic flow is not considered. Ultrasonic vibrations applied to the workpiece may help in dispersing the debris from the machining zone. But this effect has not been considered in the model.

However, finally, the model depicts the trend of machining with increase in spindle speed fairly well.

CHAPTER 7

TIME SERIES ANALYSIS OF THE CUTTING FORCE

7.1. Objective

To gain understanding of the material removal mechanism under different machining conditions, behavior of the cutting forces was analyzed using data dependent systems approach. The causes for the variations in the force profiles were analyzed. The information thus obtained could be used for online monitoring and control of the process.

7.2. Description of the data

The force signals under different machining conditions are used for the analysis. A constant feedrate of 0.13 μm/s was used for machining at spindle speeds of 500 RPM, 1000 RPM and 3000 RPM. A tool with abrasive grit size 50 μm was used for machining. A silicon wafer (Si <1 1 1>, 0.1g) was used as a workpiece. 250 data points were used each with an interval of 200 milliseconds for the analysis as shown in Figure 7.1.

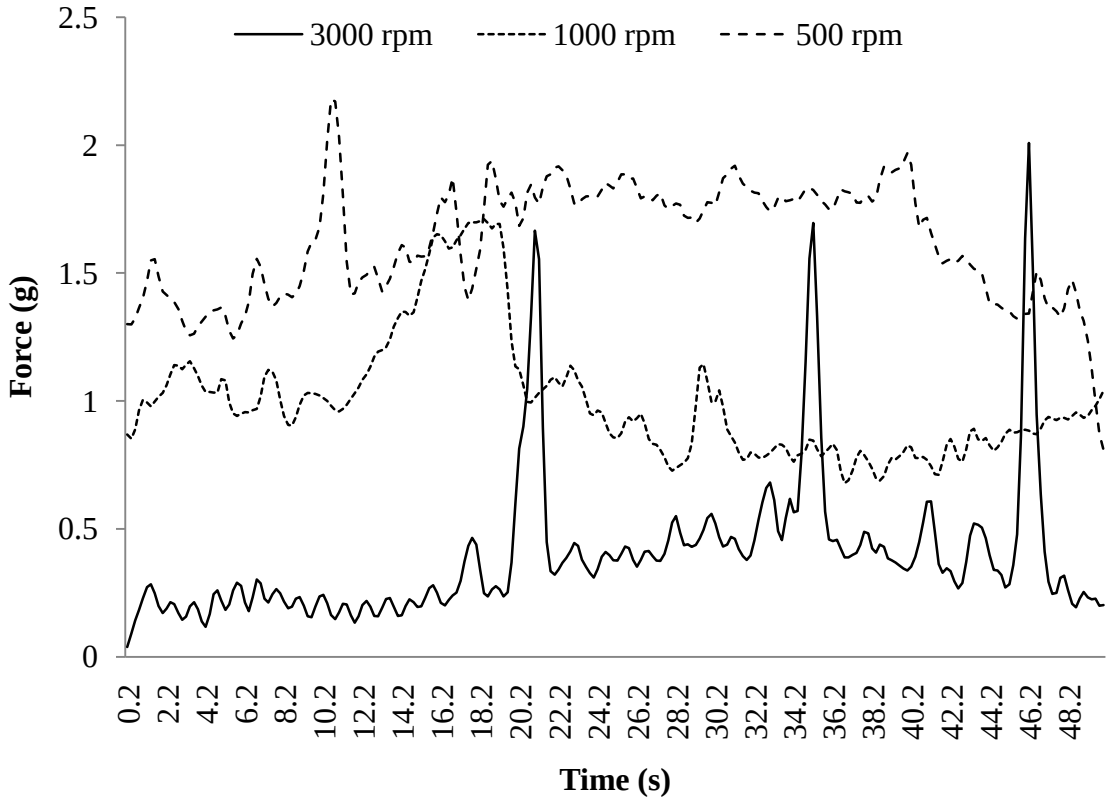

Figure 7.1. Profiles of the normal force at different spindle speeds

As the tool approaches the workpiece with a constant feedrate, the material is removed from the workpiece. The normal force is recorded after every 200 milliseconds. The variations in force signal are caused due to disturbances arising from the experimental system and the process itself. The experimental system causes variations due to the lateral vibrations induced along with the longitudinal ultrasonic vibrations. The variations because of the process are due to the impact, grinding and other modes of material removal.

7.3. Modeling

ARMA (2, 1) model was found to be adequate to fit the force data using Data Dependent Systems. Characteristic roots (λ_i), coefficients of green's function (g_i), variance component (d_i) of the ARMA (2, 1) model for the force profiles under different experimental conditions are presented in Table 7.1. The natural frequency (ω_n) and damping ratio (ζ) for the system were determined which were used to calculate the coefficients (a_0 and a_1) for the differential equations.

Table 7.1. Characteristics of ARMA (2, 1) model

Experimental Conditions	**Si (λ_i)**	**g_i**	**d_i**	**A(2)**			
				ζ	**ω_n(rad/s)**	**a_0**	**a_1**
3000 RPM	0.7107	-39.4273	-285.702	0.6277	1.5361	2.359603	1.92842
	0.7525	40.4273	342.2403				
1000 RPM	0.4421	-2.5559	-7.7471	2.1623	0.824	0.678976	3.56347
	0.9663	3.5559	174.9611				
500 RPM	0.4386	-2.5058	-7.5033	2.2726	0.7935	0.629642	3.606616
	0.969	3.5058	186.1172				

The differential equations for the system under different spindle speeds can be expressed as in Equations 7.1 - 7.3.

For 3000 RPM

$$\frac{d^2X(t)}{dt^2} + 1.9284\ \frac{dX(t)}{dt} + 2.3596\ X(t) = Z(t) \quad (7.1)$$

For 1000 RPM

$$\frac{d^2X(t)}{dt^2} + 3.5635\ \frac{dX(t)}{dt} + 0.679\ X(t)\ = Z(t) \quad (7.2)$$

For 500 RPM

$$\frac{d^2X(t)}{dt^2} + 3.6066\ \frac{dX(t)}{dt} + 0.63\ X(t) = Z(t) \qquad (7.3)$$

The Green's functions for the three spindle speeds are plotted in Figure 7.2.

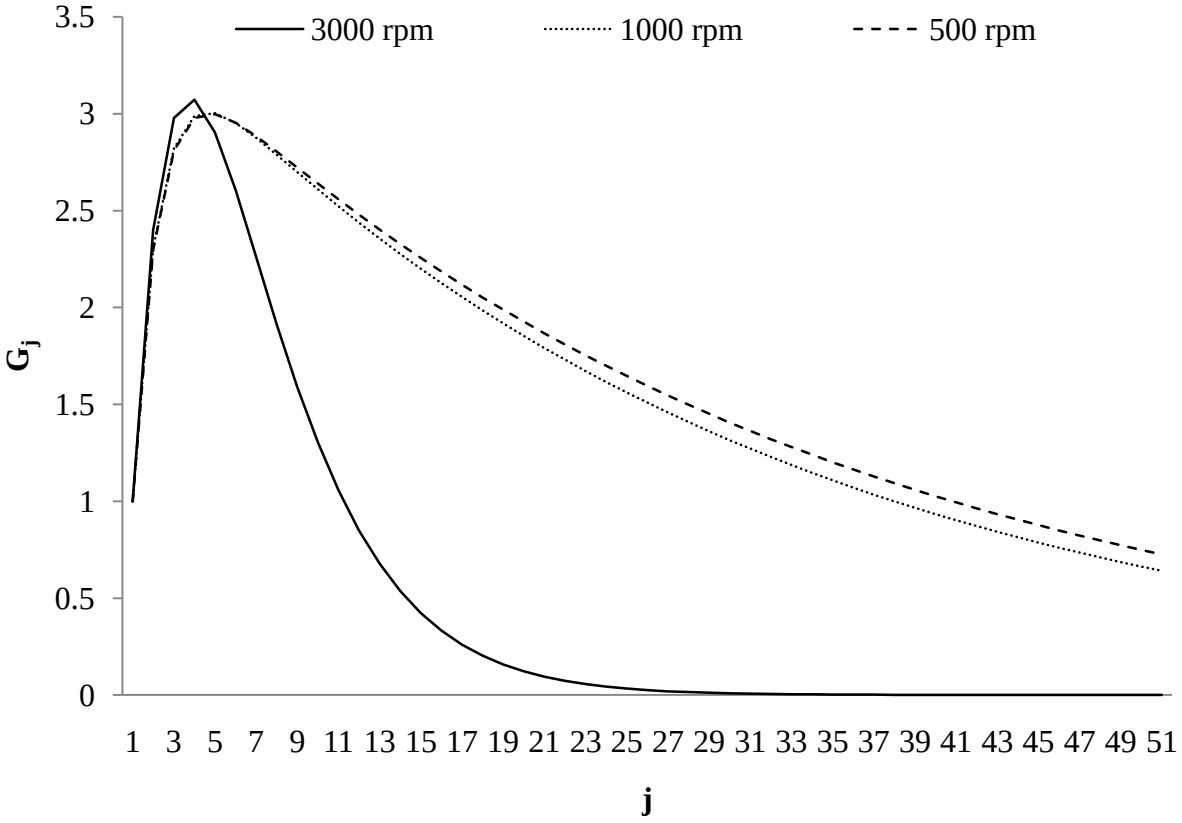

Figure 7.2. Plot of Green's functions for force at spindle speeds of 500 RPM, 1000 RPM and 3000 RPM

The plots show that the effect of the disturbances induced in the system when the spindle speed is 500 RPM lasts longer followed by the spindle speed of 1000 RPM. At a spindle speed of 3000 RPM the disturbances die out the fastest. This implies that the dependence of the force on its previous values is the least in case of highest spindle speed followed by the lower spindle speeds.

The variance calculated for the system under the three conditions is plotted in Figure 7.3 The variance is the highest for the lowest spindle speed and the lowest for the highest spindle speed.

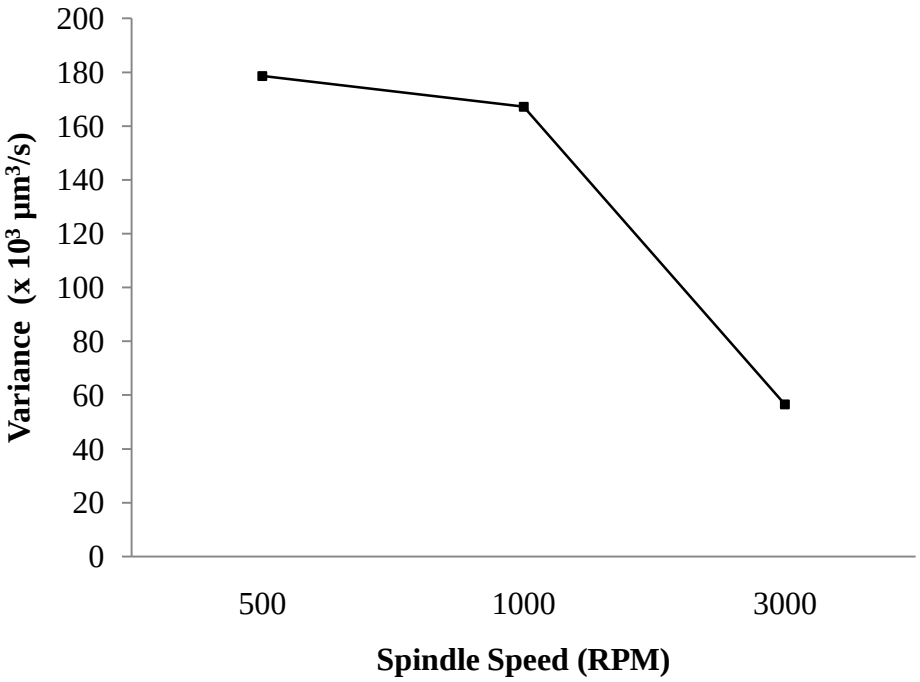

Figure 7.3. Variance of the normal machining force at different spindle speeds

7.4. Conclusion

The Green's function plot and the variance plot suggest that inspite of the occasional sharp peaks in the force at higher speed, the stability of the system is better at the higher speed.

CHAPTER 8

SUMMARY, CONCLUSIONS AND RECOMMENDATIONS

8.1. Summary and Conclusions

8.1.1. Summary

The thesis presents a feasibility study of micro rotary ultrasonic machining (MRUM) followed by an extensive experimental investigation. Rotary Ultrasonic Machining (RUM) was successfully scaled down to micro RUM. Experiments were conducted to explore the feasibility of micro rotary ultrasonic machining. Three different tools including in-house made tool, Polycrystalline diamond (PCD) tool and abrasive bonded tools were successively tried for MRUM. The feasibility study was conducted using the PCD tool. Electroplated abrasive tools could be successfully used to generate the micro holes in silicon wafers. Machinability of bone using MRUM technique was investigated. Time series analysis was used to model the behavior of the cutting force. Finally, a predictive model for estimating the material removal rate in MRUM was presented.

8.1.2. Conclusions

- The effect of tool diameter, static load, abrasive size and spindle speed on drilling speed was studied in the feasibility study conducted using the PCD tool. A larger tool diameter, higher static load, and larger abrasive size led to a higher drilling speed. Spindle speed did not affect the drilling speed significantly.
- No measureable tool wear was noticed except localized pitting. Causes for this pitting and quantification of the same need further investigation.

- The surface roughness (R_t) of the machined surface was found to be in the range of 0.3 - 0.8 µm for a sampling length of 0.08 mm.
- Even though very high quality surface finish was obtained with minimum tool wear, abrasive slurry was along with the abrasive tool for machining. Therefore, experiments were conducted using tools with larger abrasives.
- The MRR was found to increase with spindle speed, vibration amplitude and decrease in abrasive grit size when electroplated abrasive tools were used. Preliminary experiments conducted showed that MRR was higher for the cylindrical tool than for the conical tool. A higher static load and spindle speed resulted in higher MRR but also a greater hole enlargement. Therefore an optimal operating value needs to be found. The use of different coolants did not affect the MRR.
- A medium grit tool wore out faster compared to a super fine grit tool. Tool wear in the form of grain pull out and grain fracture was observed.
- The machined surface was rougher compared to the surface roughness obtained during machining using PCD tool. High wear resistance and high hardness of the PCD tool was responsible for the negligible tool wear and hence a good surface finish compared to the abrasive tools used for machining.
- Both constant feedrate and constant pressure modes were used for machining with abrasive bonded tools. Feed control is beneficial as it can be used to control the depth of indentation of the abrasives by limiting the feedrate to a small value. Consequently, machining in ductile regime can be achieved by monitoring the cutting force signal. However, employing constant feedrate mode to achieve this

objective was not possible with the existing MRUM setup because of the low sampling frequency (5 Hz) of the force sensor as well as the low torsional and longitudinal stiffness of the transducer and the force sensor respectively.

- It was concluded that as the feedrate was increased the axial forces developed also increased. The cutting forces were lowered at higher spindle speeds.
- A predictive model was developed for estimating the material removal rate. The experimental and theoretical results seemed to correlate fairly well.

Finally, a summary of the trends observed in material removal rate based on the experiments conducted in this thesis is given in Table 8.1. The shaded elements of this table give the individual effects of each of the parameters. The other elements give the combined effects of the parameters mentioned. The cross (x) indicates that the combined effects of these parameters were not evaluated experimentally during this project.

Table 8.1. Summary of the effect of parameters on the material removal rate

	Abrasive grit size	**Spindle speed**	**Vibration amplitude**	**Static load**	**Tool diameter**	**Tool shape**	**Workpiece**	**Coolant**
Abrasive grit size	↓abrasive size ↑MRR							
Spindle speed	act independently	↑spindle speed ↑MRR						
Vibration amplitude	significant interaction effect	significant interaction effect	↑vibration amp ↑MRR					
Static load	x	act independently	x	↑static load ↑MRR				
Tool diameter	x	x	x	significant interaction effect	↑tool diameter ↑MRR			
Tool shape	x	act independently	x	x	x			
Workpiece	significant interaction effect	act independently	x	x	x	x		
Coolant	x	x	x	x	x	x	x	no significant effect

8.2. Recommendations for Future Work

1) System design

- Simple cylindrical and conical tools were used for this research. Depending on the application, different shapes and lengths of the tools can be designed to obtain optimal performance in terms of material removal rate, tool wear and surface roughness.
- On one hand a very low stiffness of the machine tool deteriorates the accuracy of machining and on the other a very high stiffness might lead to excessive tool wear and induce deeper cracks in the workpiece. Therefore, designing the torsional and longitudinal stiffness of the machine tool is important.

2) **Ductile brittle transition**

- Machining under ductile regime leads to a superior surface finish and low subsurface damage. Brittle machining provides a high machining speed as opposed to ductile machining. By experimentation machining conditions that favor ductile machining and those that favor brittle machining can be identified.
- By providing online control of these parameters, transition from brittle to ductile mode of machining can be controlled as desired. For example, during deep hole drilling high speed brittle machining is more useful at the beginning and the surface finish of the hole becomes important only towards the end of machining. Therefore, brittle machining could be employed at the beginning. Using ductile machining towards the end of machining can provide better surface finish, thus eliminating the need of some finishing process steps.

3) **Tool wear monitoring and control**

- Micro tools suffer from severe tool wear problem. Therefore, for maintaining machining quality and efficiency, development of effective tool wear compensation strategies is crucial. The process signals such as grinding force, acoustic emission signals, system vibrations and spindle load individually or as combinations can be utilized for monitoring and control.

4) **Machining temperature**

- A formal investigation on the thermal aspect of RUM has not been conducted. Such an analysis can help determine if MRUM can be used for machining materials like bone which damage on exposure to high temperature.

- The temperature distribution in the machining zone might give some information on the mechanism of the material removal mechanism. For example, higher temperature might be an indication of material removal by plastic flow.

5) Parametric studies

- Exhaustive experimental studies involving more process parameters, particularly those which were not considered in this study, need to be conducted. Influence of process parameters on other performance measures of MRUM such as surface roughness, dimensional accuracy, tool wear should be studied. Such studies can enrich the existing knowledge base about the MRUM characteristics.

6) Flushing system

- Machining efficiency and repeatability can be improved by designing and employing an effective flushing system for debris removal.

7) Spindle speed control

- Spindle speed was found to influence the MRR significantly. A feedback control could be employed to ensure a constant spindle speed.

REFERENCES

1. Rajurkar, K. P., (2006). “Overview of Micromachining: Current Processes and Techniques,” SME Micro-Manufacturing Conference.
2. McGeough, J., (2002). “Micro Machining of Engineering Materials,” Marcel Dekker, Inc.
3. Sundaram, M. M., A. Sarwade, K. Rachuri, K. P. Rajurkar (2009). “Micro Rotary Ultrasonic Machining.” Transactions of the North American Manufacturing Research Institution of SME, vol. 37, pp. 621-628.
4. Churi, N. J., Z. J. Pei, C. Treadwell (2006). “Rotary Ultrasonic Machining of Titanium Alloy: Effects of Machining Variables,” Material Science and Technology: An International Journal, vol. 10, pp. 301-321.
5. Jiao, Y., P. Hu, Z. J. Pei, C. Treadwell (2005). “Rotary Ultrasonic Machining of Ceramics: Design of Experiments,” International Journal of Manufacturing Technology and Management, vol. 7, pp. 192-206.
6. Zhang, Q. H., C. L. Wu, J. L. Sun (2000). “The Mechanism of Material Removal in Ultrasonic Drilling of Engineering Ceramics,” Proceedings of the Institution of Mechanical Engineers, Part B: Journal of Engineering Manufacture, vol. 214, pp. 805-810.
7. Tyrrell, W. R., (1970), “Rotary Ultrasonic Machining,” SME Technical Paper MR70-516.

8. Khanna, N., Z. J. Pei, P. M. Ferreira (1995). “An Experimental Investigation of Rotary Ultrasonic Grinding of Ceramics Disk,” Technical Papers of The North American Manufacturing Research Institution of SME, pp. 67–72.
9. Li, Z. C. , Y. Jiao, T. W. Deines, Z. J. Pei, C. Treadwell (2005). “Rotary Ultrasonic Machining of Ceramic Matrix Composites: Feasibility Study and Designed Experiments,” International Journal of Machine Tools and Manufacture, vol. 45, pp. 1402-1411.
10. Tyrrell, W. R., (1970). “New Method for Machining Hard and Brittle Material,” SAMPE Quarterly, vol.1, pp. 55-59.
11. Kuo, K. L., (2008). “A Study of Glass Milling using Rotary Ultrasonic Machining,” Key Engineering Materials, vol. 364-366, pp. 624-628.
12. Li, Z. C. , Y. Jiao, T. W. Deines, (2004). “Experimental Study on Rotary Ultrasonic Machining (RUM) of Polycrystalline Diamond Compacts (PDC),” CD-ROM Proceedings of the 13th Annual Industrial Engineering Research Conference, Houston, TX, May 15-19.
13. Churi, N. J., Z. J. Pei, D. C. Shorter, C. Treadwell (2007). “Rotary Ultrasonic Machining of Silicon Carbide: Designed Experiments,” International Journal of Manufacturing Technology and Management, vol. 12, pp. 284-298.
14. Pei, Z. J., P. M. Ferreira, S. G. Kapoor, M. Haselkorn (1995). “Rotary Ultrasonic Machining for Face Milling of Ceramics,” International Journal of Machine Tools and Manufacture, vol. 35, pp. 1033–1046.

15. Pei, Z. J., P. M. Ferreira, M. Haselkorn (1995). “Plastic Flow in Rotary Ultrasonic Machining of Ceramics,” Journal of Material Processing Technology, vol. 48, pp. 771-777.
16. Pei, Z. J., and P. M. Ferreira (1998). “Modeling of Ductile-mode Material Removal in Rotary Ultrasonic Machining,” International Journal of Machine Tools and Manufacture, Vol. 38, pp. 1399-1418.
17. Cong, W., Z. J. Pei, N. J. Churi, Q. Wang (2009). “Rotary Ultrasonic Machining of Stainless Steel: Design of Experiments.” Transactions of North American Manufacturing Research Conference, vol. 37, pp. 261–268.
18. Pei, Z. J., N. Khanna, P. M. Ferreira (1995). “Rotary Ultrasonic Machining of Structural Ceramics: A Review,” Ceramic Engineering and Science Proceedings, vol. 16, pp. 259-278.
19. Petrukha, P. G., (1970). “Ultrasonic Diamond Drilling of Deep Holes in Brittle Materials,” Russian Engineering Journal, vol. 50, pp. 70-74.
20. Qin, N., Z. J. Pei, C. Treadwell, D. M. Guo (2009). “Physics-based Predictive Cutting Force Model in Ultrasonic-Vibration-Assisted Grinding for Titanium Drilling,” Journal of Manufacturing Science and Engineering, vol. 131, pp. 041011(1-9).
21. www.bullen-ultrasonics.com/UltraMachine.html (09/11/09).
22. www.scribd.com/doc/14370435/Advanced-Machining-ProcessHassan-E-Hofi (09/11/09).
23. Pei, Z. J., P. M. Ferreira (1999). “An Experimental Investigation of Rotary Ultrasonic Face Milling,” International Journal of Machine Tools and Manufacture, vol. 39, pp. 1327-1344.

24. Khanna, N., Z. J. Pei, P. M. Ferreira (1995). “An Experimental Investigation of Rotary Ultrasonic Grinding of Ceramics Disk,” Technical Papers of The North American Manufacturing Research Institution of SME, pp. 67–72.
25. Uhlmann, E., G. Spur, S. E. Holl (1999). “Machining of Complex Contours by Ultrasonic Assisted Grinding,” SME Technical Paper MR99-284, Society of Manufacturing Engineers, Dearborn, MI
26. Zeng, W. M., X. Xu, Z. J. Pei, (2006). “Rotary Ultrasonic Machining of Advanced Ceramics,” Materials Science Forum, vol. 532-533, pp. 361-364.
27. Zhang, Q. H., J.H. Zhang, D. M. Sun, G. D. Wang (2002). “Study on the Diamond Tool Drilling of Engineering Ceramics,” Journal of Materials Processing Technology, vol. 122, pp. 232-236.
28. Chao, C. L., W. C. Chou, C. W. Chao, C. C. Chen (2007). “Material Removal Mechanisms Involved in Rotary Ultrasonic Machining of Brittle Materials,” Key Engineering Materials, vol. 139, pp. 391-396.
29. Kuo, K. L., (2007). “Experimental Investigation of Brittle Material Milling Using Rotary Ultrasonic Machining,” Proceedings of the 35th International MATADOR Conference, Springer London, vol. 10, pp.195-198.
30. Marinescu, I., (2006). “Handbook of Advanced Ceramics Machining,” CRC Press.
31. Venkatachalam, S., (2007). “Predictive Modeling for Ductile Machining of Brittle Materials,” PhD Dissertation, Georgia Institute of Technology.
32. Ming Zhou, X. J., B. K. A. Ngoi, J. G. K. Gan (2002). “Brittle-ductile Transition in the Diamond Cutting of Glasses with the Aid of Ultrasonic Vibration,” Journal of Materials Processing Technology, vol. 121, pp. 243-251.

33. Zhao, B., X. H. Zhang, C. S. Liu, F. Jiao, X. S. Zhu (2005). “Study of Ultrasonic Vibration Grinding Character of Nano ZrO_2 Ceramics,” Key Engineering Materials, vol. 291-292, pp. 45-50.
34. Churi, N. J., Z. J. Pei, C. Treadwell (2007). “Rotary Ultrasonic Machining of Titanium Alloy (Ti-6Al-4V): Effects of Tool Variables,” International Journal of Precision Technology, vol. 1, pp. 85-96.
35. Churi, N. J., Z. J. Pei, D. C. Shorter, C. Treadwell (2009). “Rotary ultrasonic machining of dental ceramics”, International Journal of Machining and Machinability of Materials, vol. 6, pp. 270-284.
36. Wang, Q., Z. J. Pei, H. Gao, N. J. Churi, R. Renke (2009). “Rotary Ultrasonic Machining of Potassium Dihydrogen Phosphate (KDP) Crystal: An Experimental Investigation,” International Journal of Mechatronics and Manufacturing Systems, vol. 2, pp. 414-426.
37. Markov, A. I., I. D. Ustinov (1972). “A Study of the Ultrasonic Diamond: Drilling of Non-metallic Materials,” Industrial Diamond Review, pp. 97-99.
38. Kubota, M., Y. Tamura, N. Shimamura (1977). “Ultrasonic Machining with a Diamond Impregnated Tool,” Bulletin of Japan Society of Precision Engineering, vol. 11, pp. 127-132.
39. Hu, P., J. Zhang, Y. Jiao (2003). “Experimental Investigation on Coolant Effects in Rotary Ultrasonic Machining,” Proceedings of the NSF Workshop on Research Needs in Thermal Aspects of Material Removal Processes, Still water, OK, June 10-12, pp. 340-345.

40. Zeng W. M., Z. C. Li , Z. J. Pei , C. Treadwell (2005). “Experimental Observation of Tool Wear in Rotary Ultrasonic Machining of Advanced Ceramics,” International Journal of Machine Tools & Manufacture, vol. 45, no.12-13, pp. 1468-1473.
41. Gonzalo, O., J. Etxeberria, U. Abasolo, I. Vicario (2005). “Acoustic Emission Tool Wear Monitoring: from Conventional Milling to Rotary Ultrasonic Machining,” 4th E-GLEA Meeting.
42. Jiao, Y., W. J. Liu, Z. J. Pei, X. J. Xin, C. Treadwell (2005). “Study on Edge Chipping in Rotary Ultrasonic Machining of Ceramics: An Integration of Designed Experiments and Finite Element Method Analysis,” Journal of Manufacturing Science and Engineering, vol. 127, pp. 752-758.
43. Li, Z. C., L. W. Cai, Z. J. Pei, C. Treadwell (2006). “Edge-chipping Reduction in Rotary Ultrasonic Machining of Ceramics: Finite Element Analysis and Experimental Verification,” International Journal of Machine Tools and Manufacture, vol. 46, pp. 1469-1477.
44. Legge, P., (1966). “Machining without Abrasive Slurry,” Ultrasonics, pp. 157-162.
45. Prabhakar, D., (1992). “Machining of Advanced Ceramic Materials using Rotary Ultrasonic Machining Process,” M. S. Thesis, University of Illinois at Urbana-Champaign, Champaign, IL.
46. Suzuki, K., S. Mishiro, Y. Shishido, M. Iwai, W. Mei, T. Uematsu (2007). “A Micro Ultrasonic Grinding Device with Very High Frequency and its Application,” Key Engineering Materials, vol. 39, pp. 45-50.

47. Yadava, V., A. Deoghare (2007). “Design of Horn for Rotary Ultrasonic Machining using the Finite Element Method,” International Journal of Advanced Manufacturing Technology, vol. 39, pp. 9-20.
48. Ishikawa, K., H. Suwabe, T. Nishide and M. Uneda (1998). “A Study on Combined Vibration Drilling by Ultrasonic and Low-frequency Vibrations for Hard and Brittle Materials,” Precision Engineering, vol.22, pp. 196-205.
49. Li, Z. C., Y. Jiao, T. W. Deines, Z. J. Pei, C. Treadwell (2005). “Development of an Innovative Coolant System for Rotary Ultrasonic Machining,” International Journal of Manufacturing Technology and Management, vol. 7, pp. 318-328.
50. Prabhakar, D., Z. J. Pei, P. M. Ferreira, M. Haselkorn (1993). “A Theoretical Model for Predicting Material Removal Rates in Rotary Ultrasonic Machining of Ceramics,” Transactions of the North American Manufacturing Research Institution of SME, vol. 21, pp. 167–172.
51. Ya, G., H. W. Qin, S. C. Yang (2002). “Analysis of the Rotary Ultrasonic Machining Mechanism,” Journal of Materials Processing Technology, vol. 129, pp. 182-185.
52. Hu, X., (2007). “Mechanism, Characteristics and Modeling of Micro Ultrasonic Machining,” PhD dissertation, University of Nebraska - Lincoln.
53. Yang, Y., X. Li, (2003). “Micro Ultrasonic Machining of Ceramic MEMS with Micro Metallic Dies,” IMECE, vol. 5, pp. 93-95.
54. Cherku, S., (2008). “Study of Machining Characteristics and Modeling of Micro Ultrasonic Machining,” Master of Science Thesis, University of Nebraska – Lincoln.
55. http://www.strauss-co.com/den_fg.html (11/24/2009).

56. Brehl, D. E., T. A. Dow (2008). “Review of Vibration-assisted Machining,” Precision Engineering, vol.32 (3), pp.153-172.

57. Sundaram, M. M., S. Cherku, K. P. Rajurkar (2008). “Micro Ultrasonic Machining Using Oil Based Abrasive Slurry,” ASME Technical Publication, MSEC_ICMP2008-72138.

58. Ferreira, P. M., N. Khanna, Z. J. Pei, (1997). “Rotary Ultrasonic Grinding Apparatus and Process,” United States Patent 5655956.

59. Dong, X., S. Jahanmir, L. K. Ives, E. D. Rekow (2000). “Abrasive Machining of Glass-ceramics with a Dental Handpiece,” Machining Science and Technology, vol. 4, pp. 209-233.

60. Kaburlasos, V. G., V. Petridis, P. N. Brett, D. A. Baker (1999). “Estimation of the Stapes- Bone Thickness in the Stapedotomy Surgical Procedure using a Machine-learning Technique,” IEEE Transactions of Information Technology Biomedicine, vol. 3 (4), pp. 268-277.

61. Harvey, S. A., (2003). “Stapedectomy: Laser versus Drill versus the use of Pick Instruments,” Operative Techniques in Otolaryngology-Head and Neck Surgery, Otology: Surgery for Deafness,” vol. 14 (4), pp. 255-262.

62. Brett, P. N., D. A. Baker, L. Reyes, J. Blanshard (1995). “An Automatic Technique for Micro-drilling a Stapedotomy in the Flexible Stapes Footplate,” Proceedings of the Institution of Mechanical Engineers, Part H: Journal of Engineering in Medicine, vol. 209 (4), pp. 255-62.

63. Gleizal, A., J. -C. Bera, B. Lavandier, J. -L. Beziat (2007). “Piezoelectric Osteotomy: A New Technique for Bone Surgery—Advantages in Craniofacial Surgery,” Child's Nervous System, vol. 23, pp. 509–513.

64. González-García, A., M. Diniz-Freitas, M. Somoza-Martín, A. García-García (2009). “Ultrasonic Osteotomy in Oral Surgery and Implantology,” Oral Surgery, Oral Medicine, Oral Pathology, Oral Radiology and Endodontics, vol. 108 (3), pp. 360-367.

65. Heinz-Michael, M., (2005). “Minimally Invasive Spine Surgery: A Surgical Manual,” Birkhäuser, ISBN 3540213473, 9783540213475.

66. Prabhu, K. S., (2007). “Improved Bone Drilling Process Through Modeling and Testing,” Master of Science Thesis, University of Florida.

67. Giraud, J.-Y., S. Villemin, J. Darmana, J. -Ph. Cahuzac, A. Autefage, J. –P. Morucci (1991). “Bone Cutting,” Clinical Physics and Physiological Measurement, vol.12 (1), pp. 1-19.

68. Abouzgia, M. B., D. F. James (1995). “Measurements of Shaft Speed while Drilling through Bone,” International Journal of Oral & Maxillofacial Surgery, vol. 54 (3), pp. 1315-1316.

69. Matthews, L. S., C. Hirsch (1972). “Temperatures Measured in Human Cortical Bone when Drilling,” Journal of Bone and Joint Surgery, vol. 54, pp. 297-308.

70. Bachus, K. N., M. T. Rondina, D. T. Hutchinson (2000). “The Effects of Drilling Force on Cortical Temperatures and their Duration: an in Vitro Study,” Medical Engineering & Physics, vol. 22 (10), pp. 685-91.

71. Davidson, S. R. H., D. F. James (2003). “Drilling in Bone: Modeling Heat Generation and Temperature Distribution,” Journal of Biomechanical Engineering, vol. 125 (3), pp. 305-314.

72. Natali, C., P. Ingle, J. Dowell (1996). “Orthopedic Bone Drills-Can they be Improved? Temperature Changes near the Drilling Face,” Journal of Bone and Joint Surgery - British Volume, vol. 78 (3), pp. 357-62.

73. Sugita, N., T. Osa, R. Aoki, M. Mitsuishi (2009). “A New Cutting Method for Bone Based on its Crack Propagation Characteristics,” CIRP Annals-Manufacturing Technology vol. 58, pp. 113-118.

74. Ngoi, B. K. A., P. S. Sreejith, (2000). “Ductile Regime Finish Machining - A Review,” The International Journal of Advanced Manufacturing Technology, vol. 16 (8), pp. 547-550.

75. www.imse.ksu.edu/~zpei/ultrasonic_machining/html/tutorial.htm (11/24/2009).

76. Thoe, T. B., D. K. Aspinwall, M. L. H. Wise (1998). “Review on Ultrasonic Machining,” International Journal of Machine Tools and Manufacture, vol. 38 (4), pp. 239-255.

77. Ohashi, H., M. Therin, A. Meunier, P. Christel (1994). “The Effect of Drilling Parameters on Bone,” Journal of Materials Science: Materials in Medicine, vol. 5 (4), pp. 225-231.

78. Sugita, N., F. Genma, Y. Nakajima, M. Mitsuishi, K. Fujiwara, N. Abe, T. Ozaki, M. Suzuki, H. Moriya, T. Inoue, K. Kuramoto, Y. Nakashima, K. Tanimoto (2007). “Bone Cutting Robot with Soft Tissue Collision Avoidance Capability by a

Redundant Axis for Minimally Invasive Orthopedic Surgery," IEEE/ICME International Conference on Complex Medical Engineering, pp. 48-51.

79. Sugita, N., T. Nakano, Y. Nakajima, K. Fujiwara, N. Abe, T. Ozaki, M. Suzuki, M. Mitsuishi (2009). "Dynamic Controlled Milling Process for Bone Machining," Journal of Materials Processing Technology, vol. 209 (17), pp. 5777-5784.
80. Wang, J., M. Ye, Z. Liu, C. Wang, (2009). "Precision of Cortical Bone Reconstruction Based on 3D CT Scans," Computerized Medical Imaging Graphics, vol. 33 (3), pp. 235-41.
81. Denis, K., G. Van Ham, J. Vander Sloten, R. Van Audekercke, G. Van der Perre, J. De Schutter, J.-P. Kruth, J. Bellemans, G. Fabry (2001). "Influence of Bone Milling Parameters on the Temperature Rise, Milling Forces and Surface Flatness in View of Robot-Assisted Total Knee Arthroplasty," International Congress Series, Computer Assisted Radiology and Surgery, June 1230, pp. 300-306.
82. Jackson, M. J., G. M. Robinson, H. Sein, W. Ahmed, R. Woodwards (2005). "Machining Cancellous Bone Prior to Prosthetic Implantation," Journal of Materials Engineering and Performance vol. 14, pp. 293-300.
83. Honl, M., R. Rentzsch, G. Müller, C. Brandt, A. Bluhm, E. Hille, H. Louis, M. Morlock (2000). "The use of Water-Jetting Technology in Prostheses Revision Surgery - First Results of Parameter Studies on Bone and Bone Cement," Journal of Biomedical Materials Research Part B: Applied Biomaterials, vol. 53 (6), pp. 781-790.
84. Karsten, S., C. Volker, R. Reemt, B. Axel, B. Nick, H. Ekkehard, L. Hartmut, M. Michael, H. Matthias (2004). "Abrasive Water Jet Cutting as a New Procedure for

Cutting Cancellous Bone - In Vitro Testing in Comparison with the Oscillating Saw," Journal of Biomedical Materials Research, vol. 71b (2) , pp. 223-228.

85. Wang, J., D. K. Shanmugam (2009). "Cutting Meat with Bone using an Ultrahigh Pressure Abrasive Waterjet," Meat Science, vol. 81(4), pp. 671-677.
86. Kim D, H. Owada, N. Hata, T. Dohi (2004). "An Er: YAG Laser Bone Cutting Manipulator for Precise Rotational Acetabular Osteotomy," Conf Proc IEEE Engineering in Medicine and Biology Society, vol. 4, pp. 2750-3.
87. Eyrich, G. K. H., (2005). "Laser-Osteotomy Induced Changes in Bone," Medical Laser Application, vol. 20 (1), pp. 25-36.
88. Zhang, X., S. Xie, Z. Zhan, Q. Ye (2007). "One Dimension Dynamic Ablation of Bovine Shank Bone with Pulse CO_2 Laser," Progress in Biomedical Optics and Imaging, vol. 8 (49), pp. 68260I.1-68260I.8.
89. Kuttenberger, J. J., S. Stübinger, A. Waibel, M. Werner, M. Ivanenko, P. Hering, B. von Rechenberg, R. Sader, H. F. Zeilhofer (2008). "Computer-guided CO_2-laser Osteotomy of the Sheep Tibia: Technical Prerequisites and First Results," Photomedicine and Laser Surgery, vol. 26 (2), pp. 129-136.
90. Landes, C. A., S. Stübinger, J. Rieger, B. Williger, T. K. L. Ha, R. Sader (2008). "Critical Evaluation of Piezoelectric Osteotomy in Orthognathic Surgery: Operative Technique, Blood Loss, Time Requirement, Nerve and Vessel Integrity," Journal of Oral and Maxillofacial Surgery, vol. 66 (4), pp. 657-674.
91. Ishida, S., N. Hata, T. Azuma, S. Umemura, T. Dohi (2002). "Non-invasive Osteotomy using Focused Ultrasound," Proc. of the 16th International Congress and Exibition, Computer Assisted Radiology and Surgery, Paris, 258-262.

92. Yeager, C., A. Nazari, D. Arola (2008). “Machining of Cortical Bone: Surface Texture, Surface Integrity and Cutting Forces, Machining Science and Technology,” vol. 12, pp. 100 -118.
93. Ercoli C., P. D. Funkenbusch, H. J. Lee, M. E. Moss G. N. Graser (2004). “The Influence of Drill Wear on Cutting Efficiency and Heat Production during Osteotomy Preparation for Dental Implants: A Study of Drill Durability,” International Journal of Oral & Maxillofacial Implants, vol. 19 (3), pp. 335-349.
94. Evans, A. G., D. B. Marshall (1981), “Wear Mechanisms in Ceramics,” Fundamentals of Friction and Wear of Materials (Ed. D. A. Rigney), pp.439-442.
95. http://www.physikinstrumente.com/tutorial/4_26.html